BOREAS Radar Observations and Science

Sassan Saatchi
Jet Propulsion Laboratory
California Institute of Technology
Pasadena, CA, USA

BOREAL ECOSYSTEM - ATMOSPHERE STUDY
BOREAS

Polarizations: HH, HV, VV

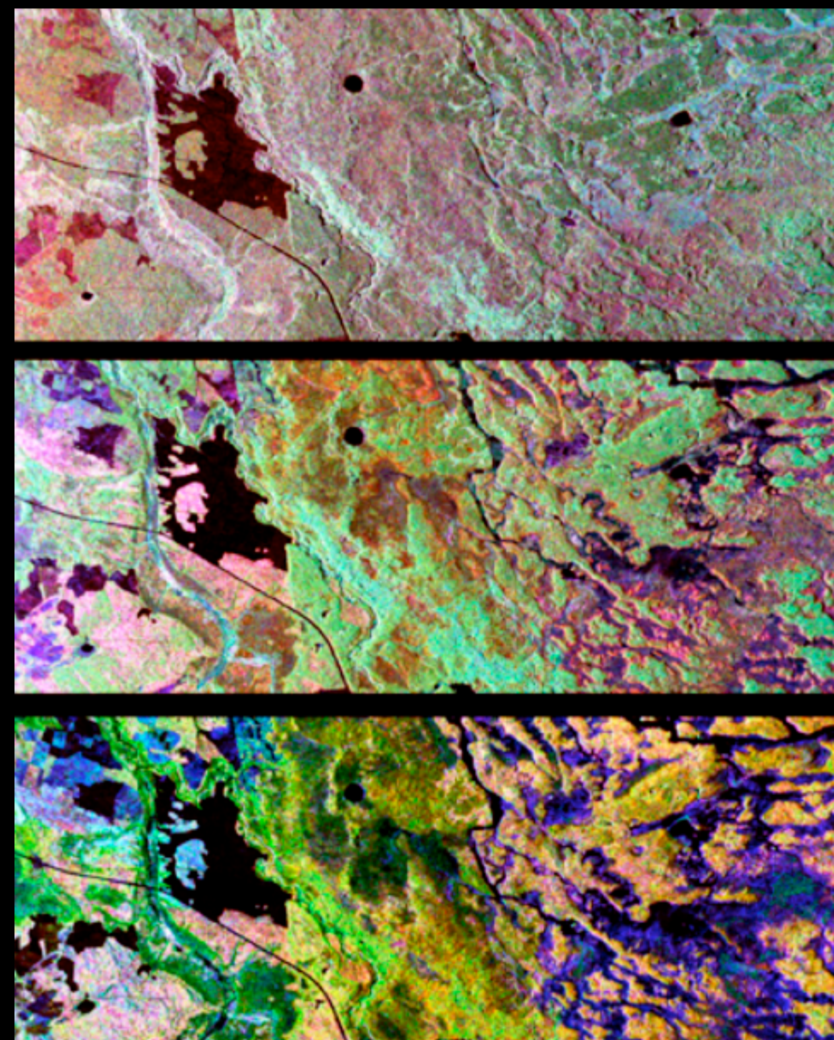

How FIFE and BOREAS Changed the World

Oct 6-7, 2016
NASA/GSFC

Outline

Overall Science Objectives and Projects

Forest Structure and Aboveground Biomass Density

Soil Moisture and Canopy Water Content

Monitoring Freeze/thaw Cycles

Overall Science Objectives and Projects

- Vegetation Structure and Biomass
- Vegetation & Soil Water Content
- Phenology and freeze/thaw

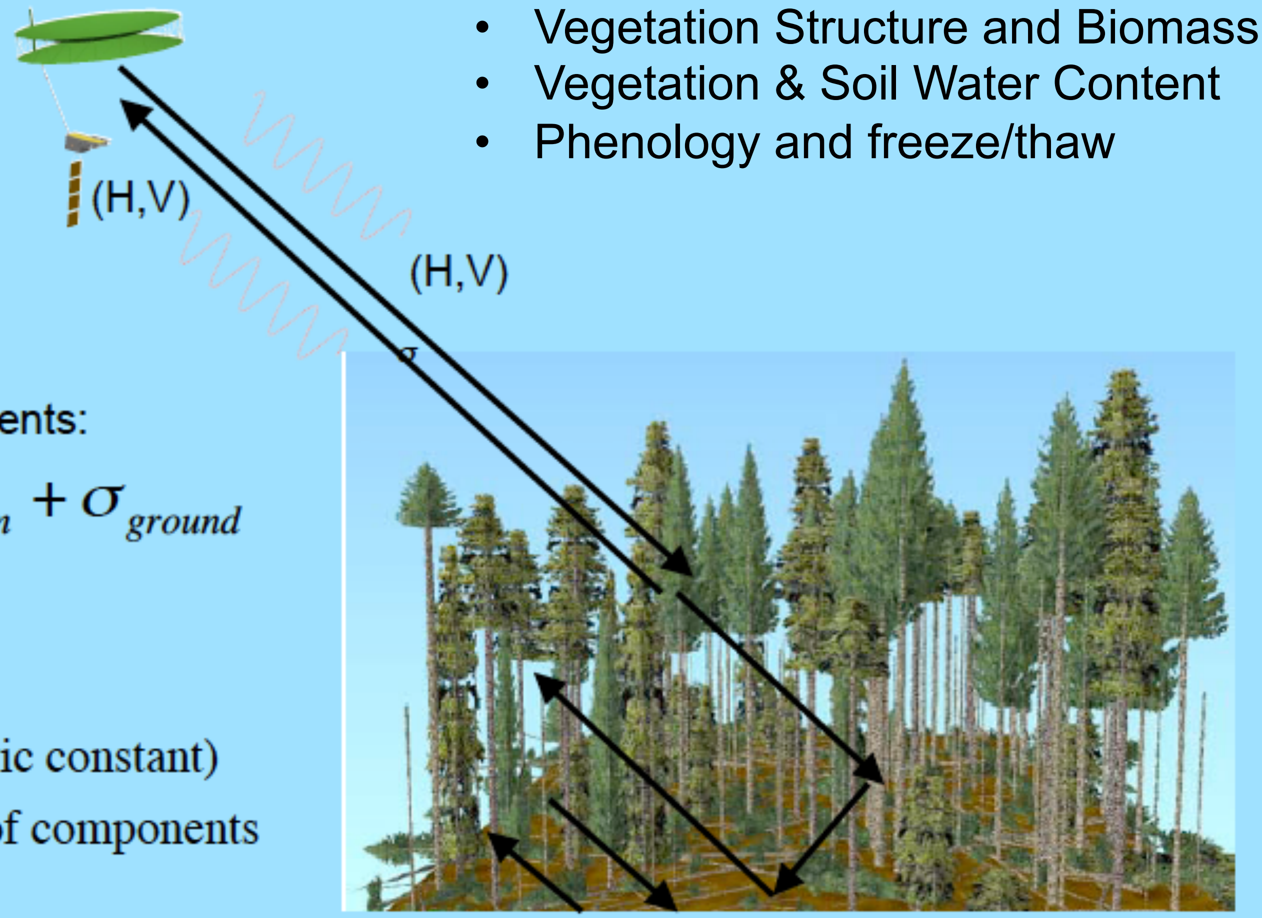

Backscatter Measurements:

$$\sigma_{(H,V)} = \sigma_{crown} + \sigma_{stem} + \sigma_{ground}$$

$\sigma_{(H,V)} = f(vol, W_d, \Omega)$

vol : forest volume (size)

W_d : wood density (dielectric constant)

Ω : shape and orientation of components

Measurement Variables: Frequency, Angle, Polarization

high spatial resolution, seasonal to annual revisit time, all time capability

BOREAS studies

RSS-13: Helicopter-Based Measurements of Microwave Scattering Over the Boreal Forest

P.I.(s): S. Prasad Gogineni -- University of Kansas

GSRP Student: G. Lance Lockhart -- University of Kansas

RSS-15: Distribution and Structure of Above Ground Biomass in Boreal Forest Ecosystems

P.I.(s): K. Jon Ranson -- NASA/Goddard Space Flight Center; Roger Lang-- George Washington University

Co-I(s): Guoqing Sun -- SSAI; Narinder Chauhan -- GWU

RSS-16: Estimation of Hydrological Parameters in Boreal Forest Using SAR Data:

P.I.(s): Sassan S. Saatchi--NASA/Jet Propulsion Laboratory

Co-I(s): Jacob van Zyl, Mahta Mogaddam -- NASA/JPL; Ted Engman -- NASA/GSFC

RSS-17: Monitoring Environmental and Phenologic State and Duration of State with SAR as Input to Improved CO_2 Flux Models

P.I.(s): JoBea Way -- NASA/Jet Propulsion Laboratory

Co-I(s): Eric Rignot, Reiner Zimmermann -- NASA/JPL; Gordon Bonan – NCAR

TE-16: Land Cover and Primary Productivity in the Boreal Forest

P.I.(s): Josef Cihlar -- Canada Center for Remote Sensing (CCRS)

Co-I(s): Zhanqing Li, Jing M. Chen -- CCRS; Raymond Desjardins -- Agriculture Canada

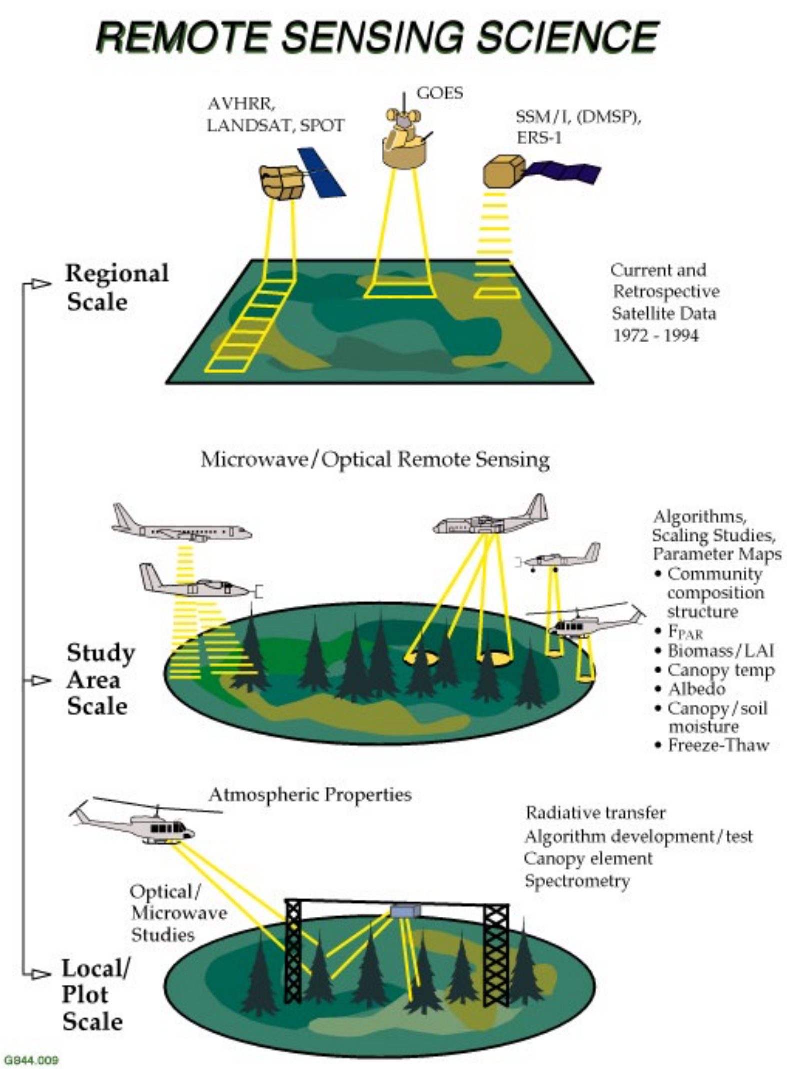

AIRSAR Team Before Deployment to BOREAS 1993

Impacts of Structure and Moisture on Radar Measurements

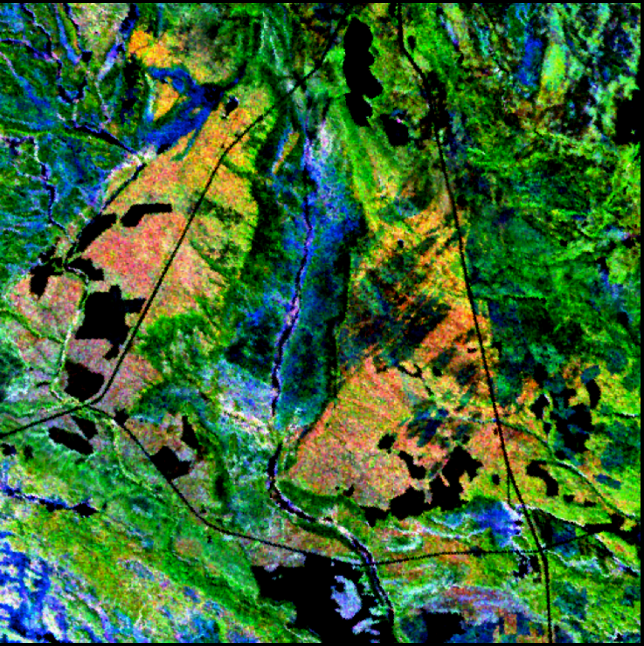

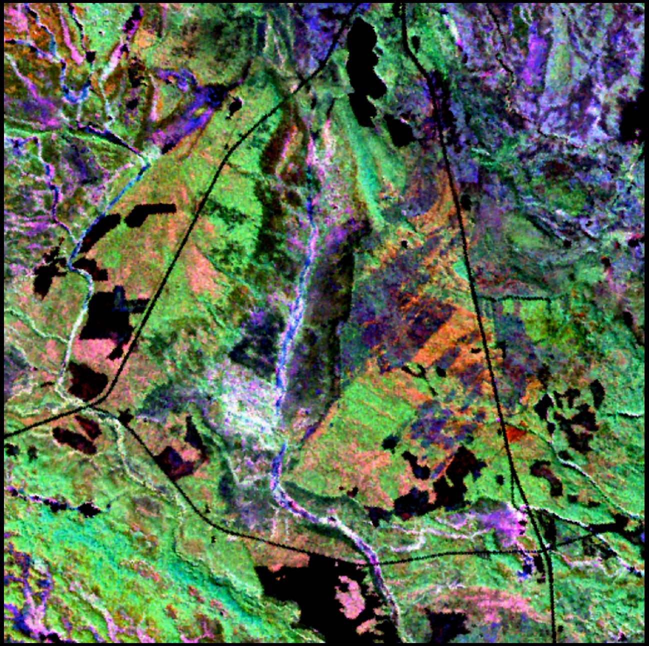

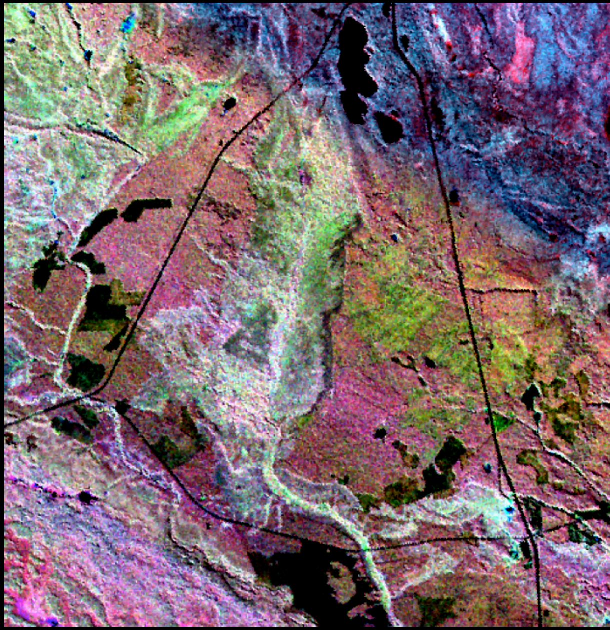

P-band (HH,HV,VV)
P-band
70 cm

L-band(HH,HV,VV)
L-band
24 cm

C-band (HH,HV,VV)
C-band
6 cm

Forest Structure & Biomass

Forest Structure & Biomass

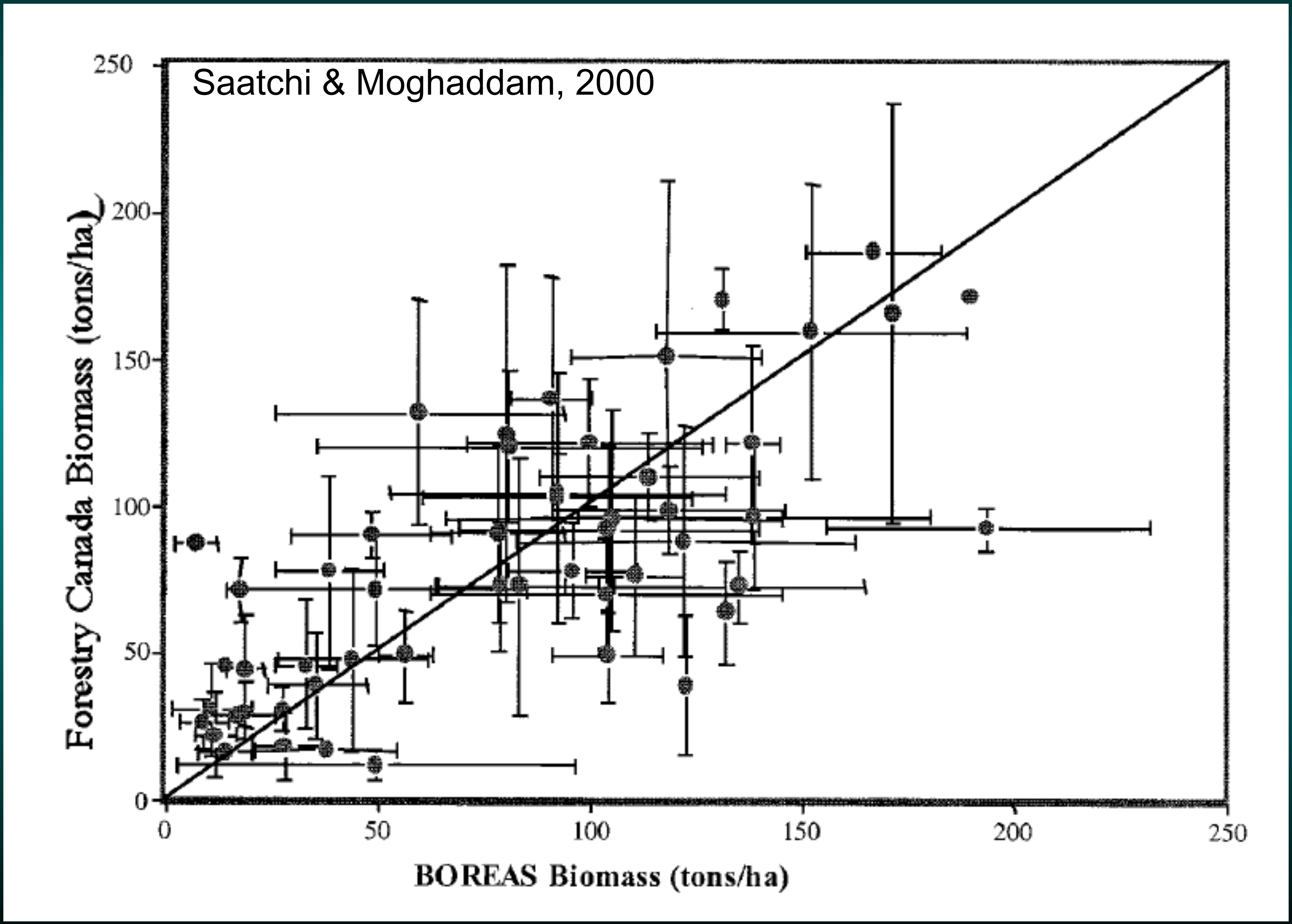

Ecosystem Biomass Algorithm Theoretical Basis

- L-band backscatter sensitivity to aboveground forest biomass have been studied over the past 30 years
- L-band radar backscatter is dominated by three scattering terms: volume, volume-surface, and surface
- L-band HV backscatter has strong sensitivity to AGB up to ~100 Mg/ha with low to moderate impacts of soil moisture compared to co-polarization channels.
- The algorithm is based on a physically based EM model with reduced parameters to include biomass, soil moisture, and roughness in a semi-empirical formulation.

$$\sigma^0 = \sigma^0_{vol} + \Gamma_{surf}\sigma^0_{vol\_surf} + \Gamma_{vol}\sigma^0_{surf}$$

σ^0_{vol} : vegetation

$\sigma^0_{vol\_surf}$: vegetation

σ^0_{surf} : soil

$\Gamma_{surf} = |R|^2 \exp(-k^2 s^2 \cos^2\theta)$: soil

$\Gamma_{vol} = \exp(-2\alpha)$: vegetation

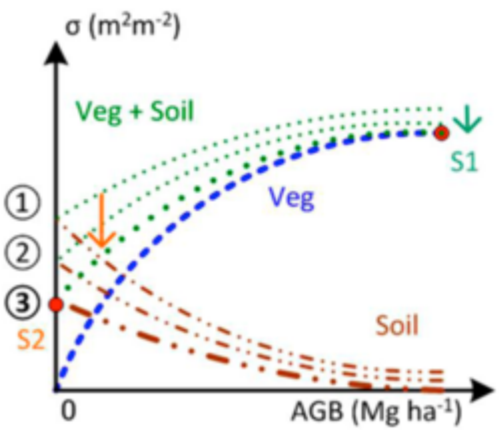

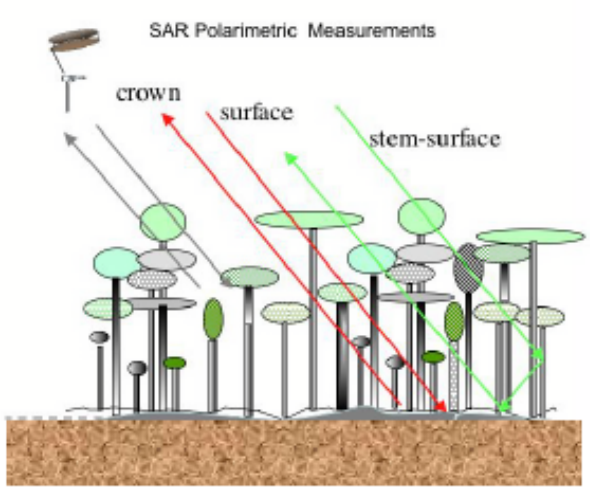

Biomass Estimation Methodology

Radar Images

Land Cover Map

Training & Validation Data Set

Semi-empirical Estimation Algorithm For Crown and Stem Biomass

Crown Biomass

Stem Biomass

Total Above Ground Biomass

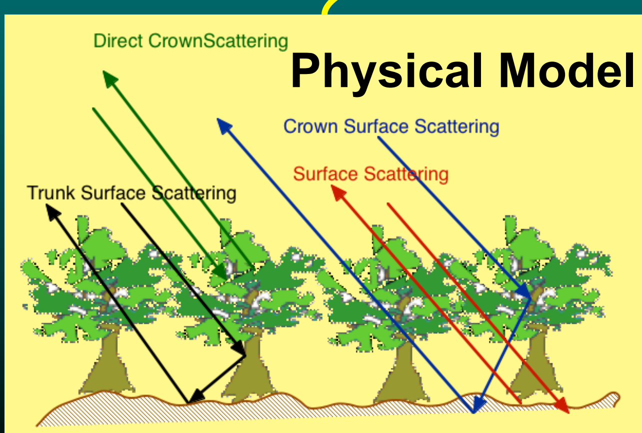

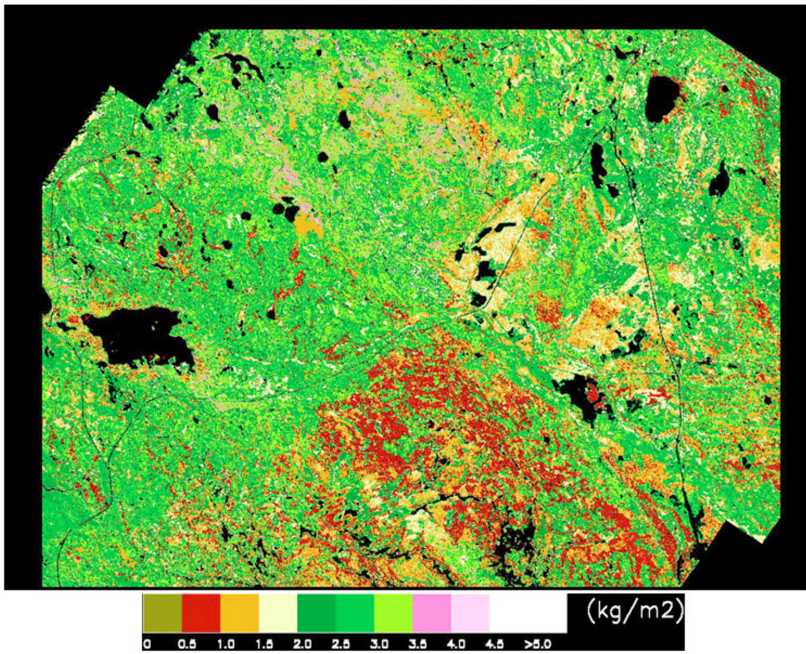
(kg/m2)
0 0.5 1.0 1.5 2.0 2.5 3.0 3.5 4.0 4.5 >5.0

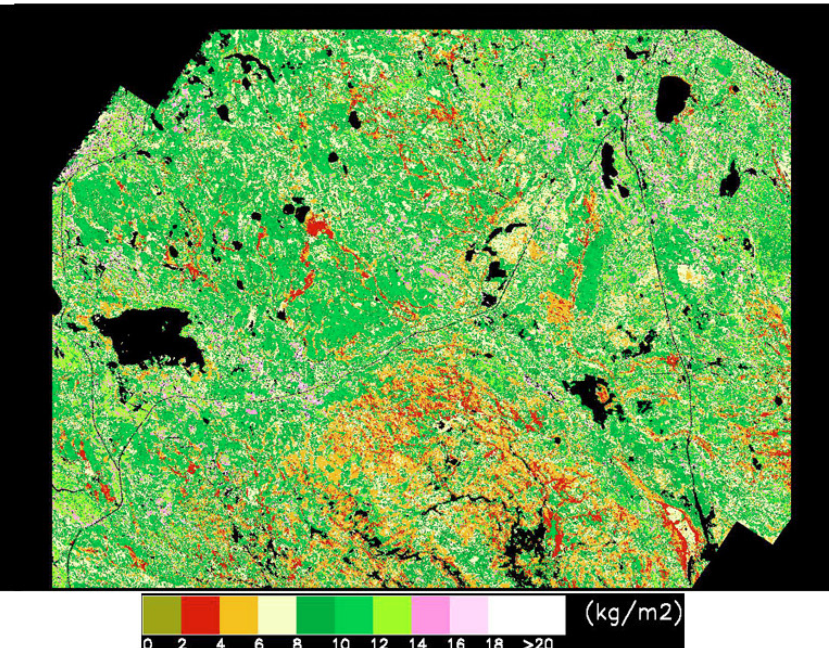
(kg/m2)
0 2 4 6 8 10 12 14 16 18 >20

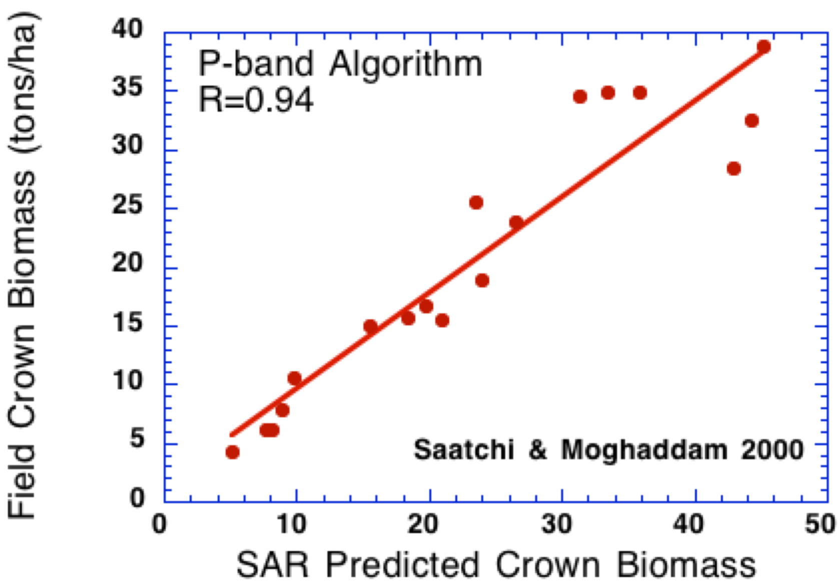
P-band Algorithm
R=0.94
Saatchi & Moghaddam 2000
Field Crown Biomass (tons/ha)
SAR Predicted Crown Biomass
0 5 10 15 20 25 30 35 40
0 10 20 30 40 50

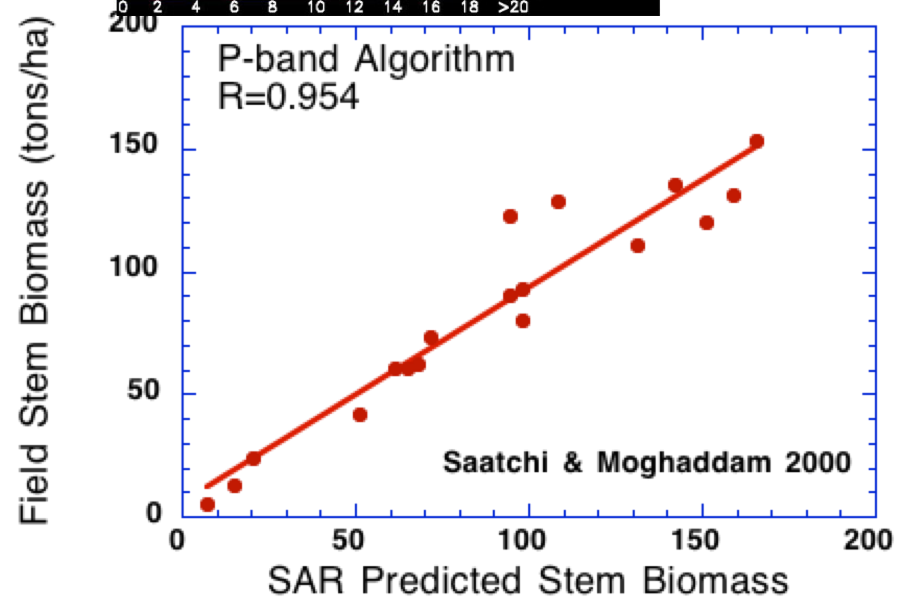
P-band Algorithm
R=0.954
Saatchi & Moghaddam 2000
Field Stem Biomass (tons/ha)
SAR Predicted Stem Biomass
0 50 100 150 200
0 50 100 150 200

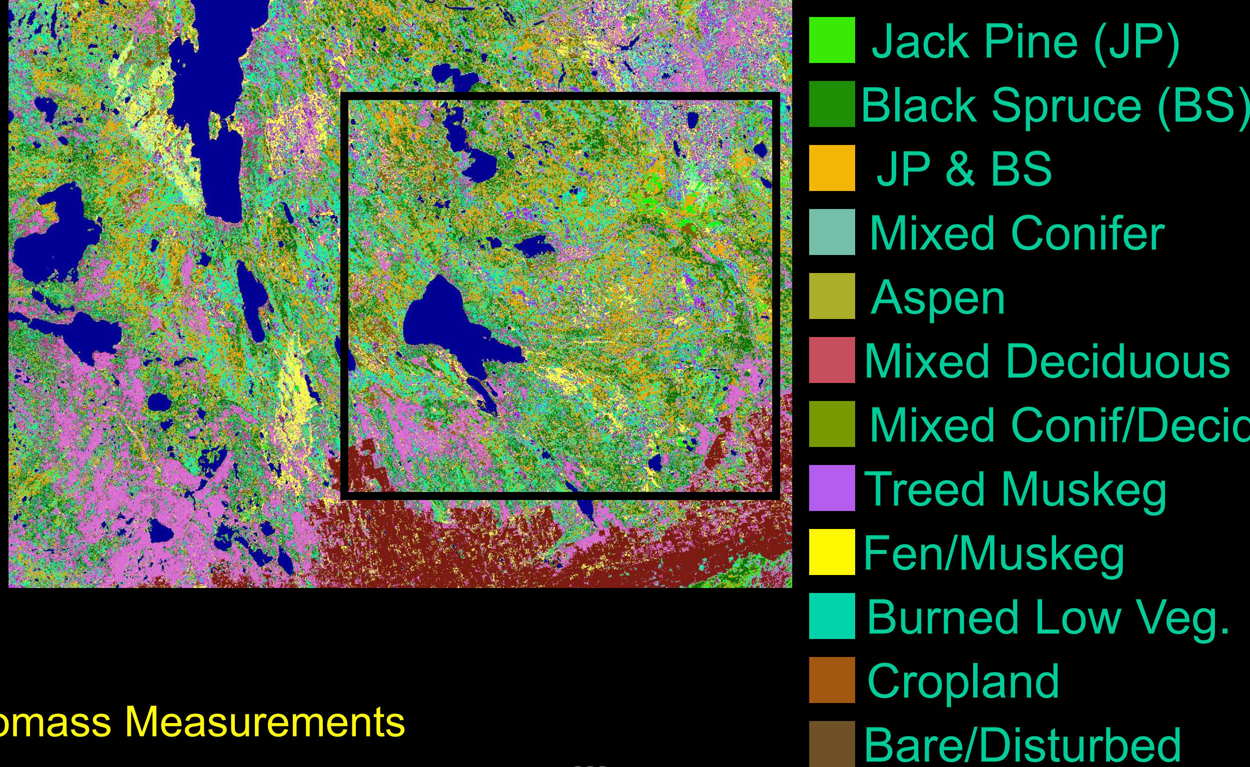

Boreal Forest Biomass Measurements

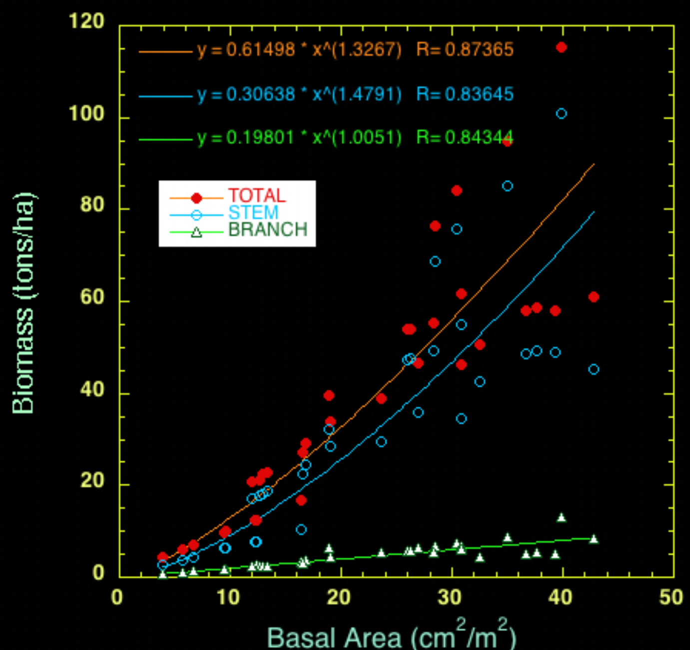

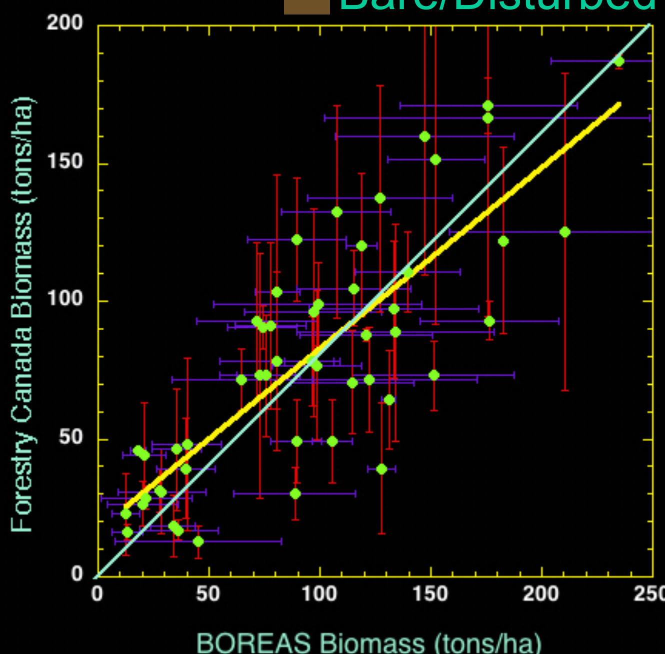

L-band Polarimetric Derived Biomass
SIR-C Observations from Shuttle Mission 1994

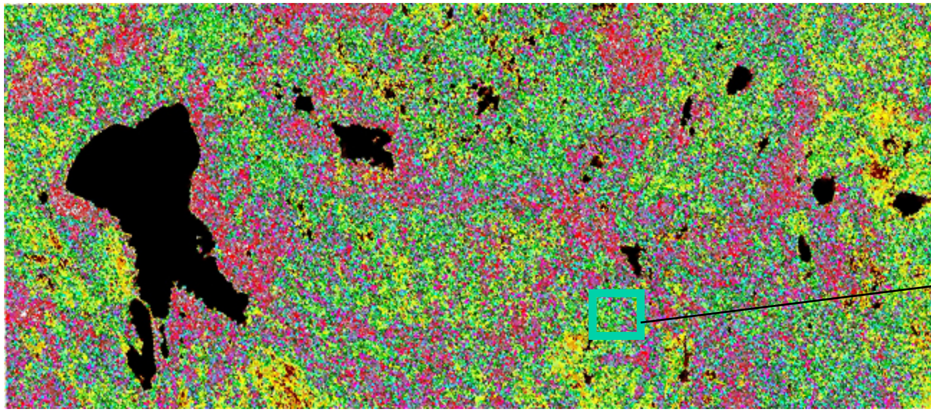

SIR-C Derived Biomass Map
(Ranson et al. 1997)

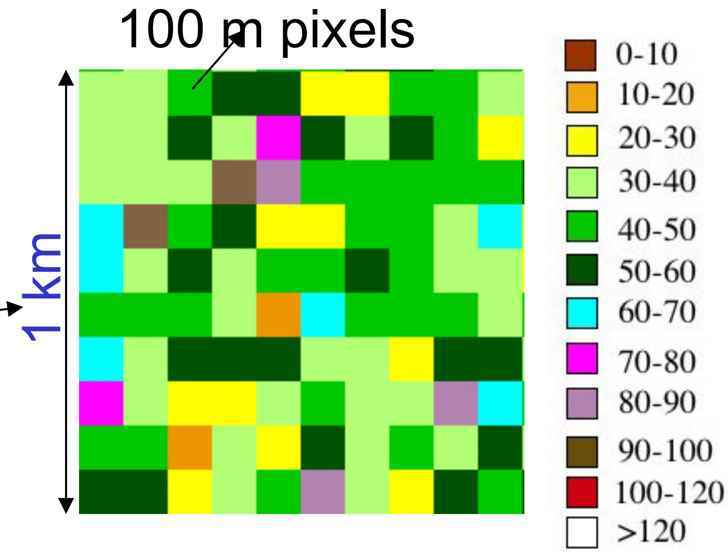

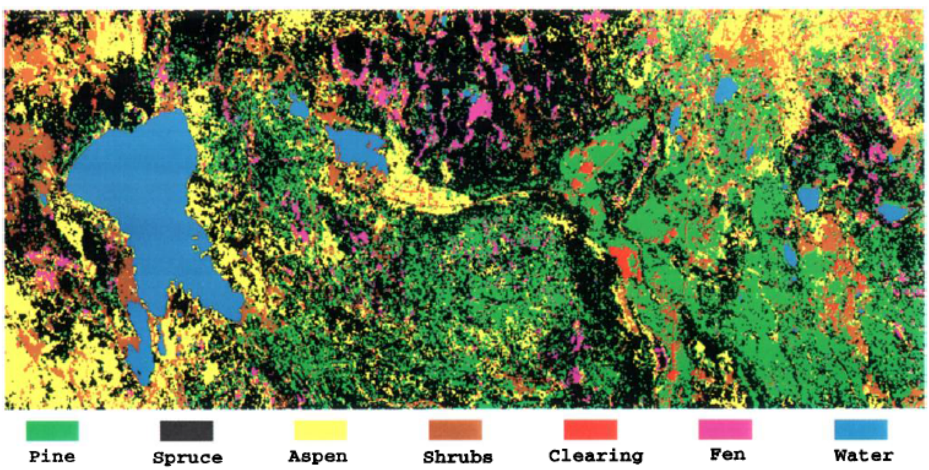

SIR-C Derived Land Cover Types
(Ranson et al. 1995)

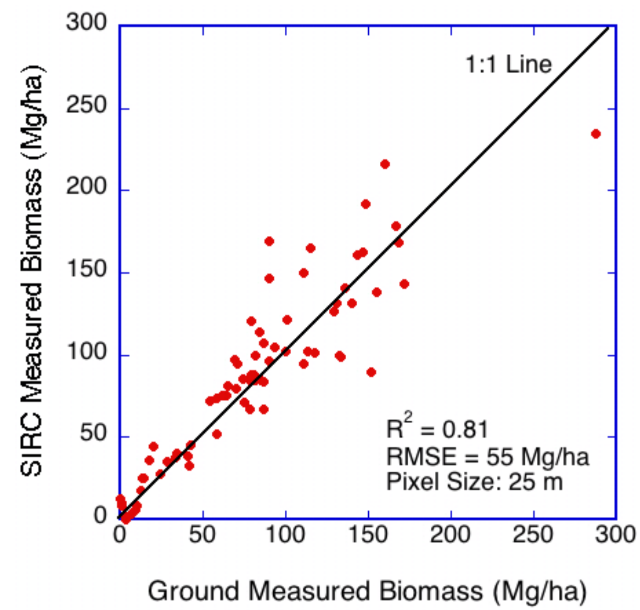

L-band Radar Sensitivity to Biomass

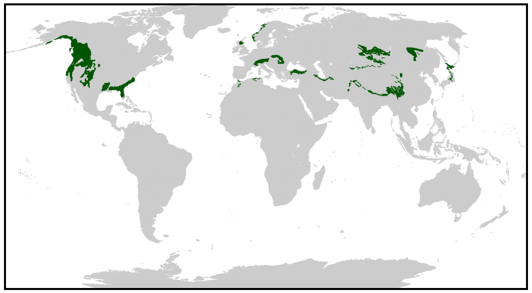

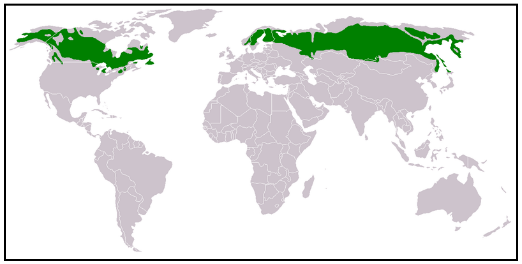

Geographic Distribution of Northern Conifers

NISAR L-band HV Backscatter Measurements Capture Spatial Variations of Biomass in boreal forests

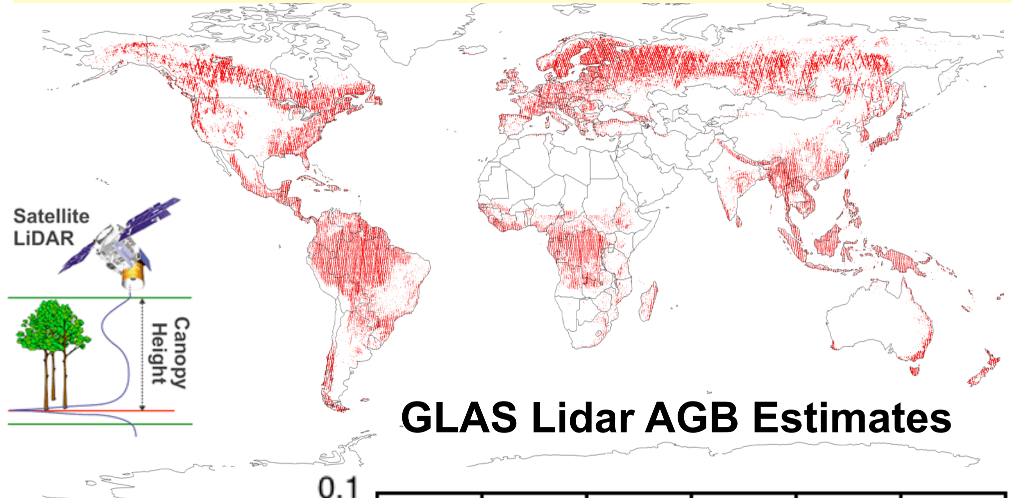

GLAS Lidar AGB Estimates

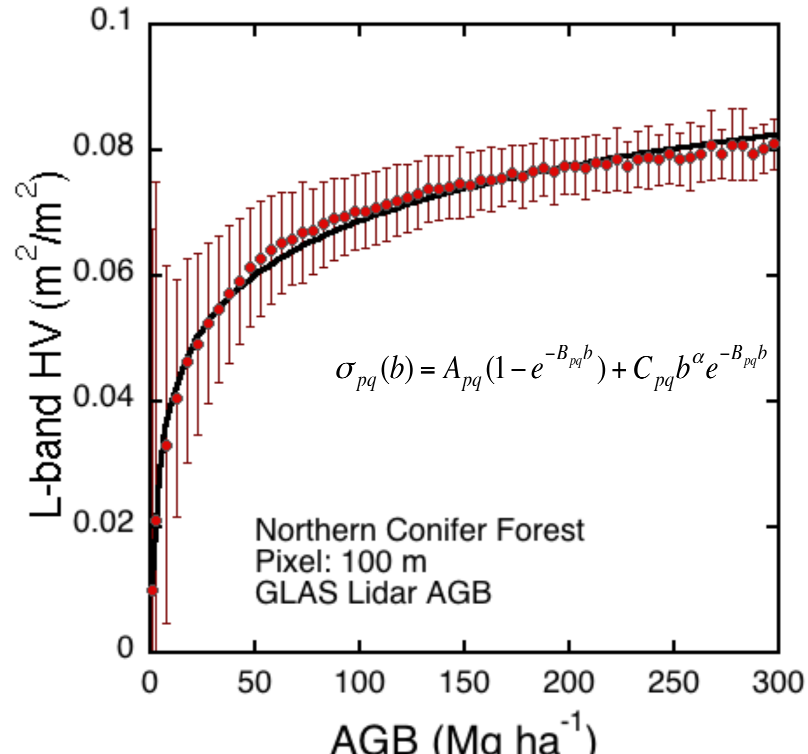

Sensitivity of boreal forest regional water flux and net primary production simulations to sub-grid-scale land cover complexity
Kimball et al. 1999

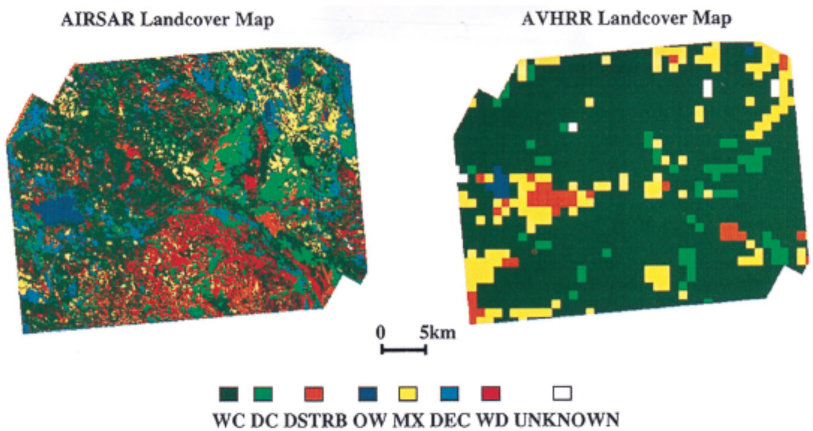

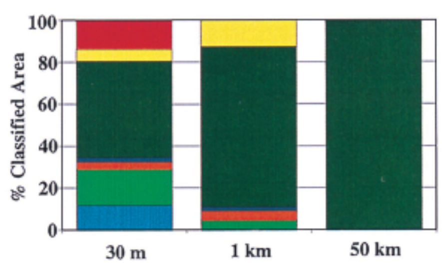

Net Primary Production
(Mg ha^{-1} yr^{-1})

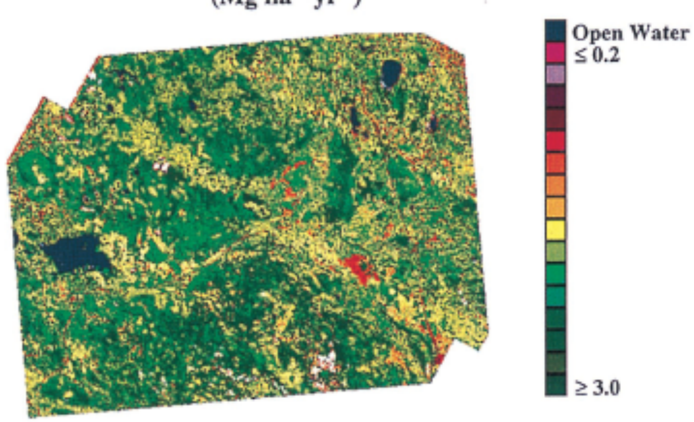

Integration of AIRSAR Derived Land Cover Map and Biomass in BIOME-BGC

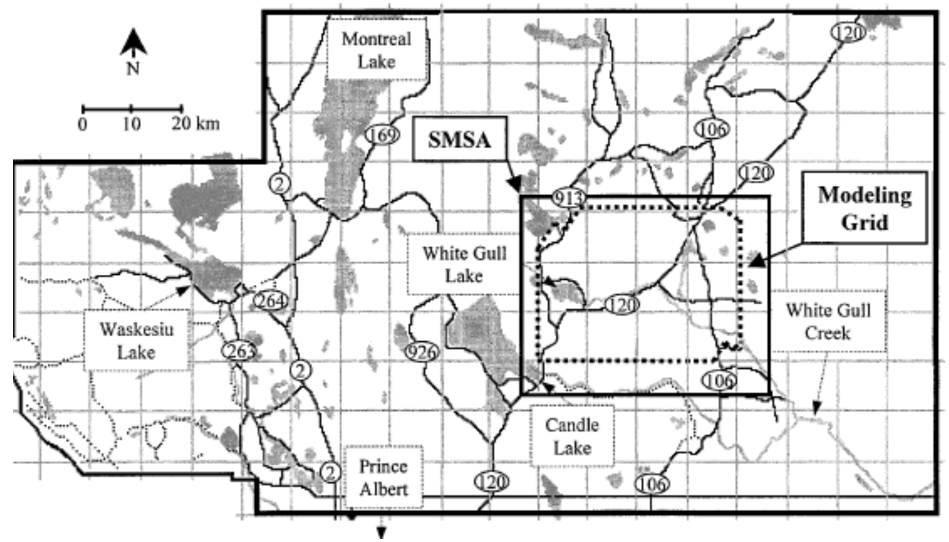

1. NPP and ET fluxes were spatially complex.
2. Biomass and LAI heterogeneity controlled the flux variability
3. Spatial aggregation caused a factor 2 bias in mean monthly NPP and a factor of 7 in annual estimation of uncertainty!

Regional assessment of boreal forest productivity using an ecological process model and remote sensing parameter maps

Kimball et al. 2000

Integration of AIRSAR Derived Land Cover Map, Biomass, and LAI in BIOME-BGC

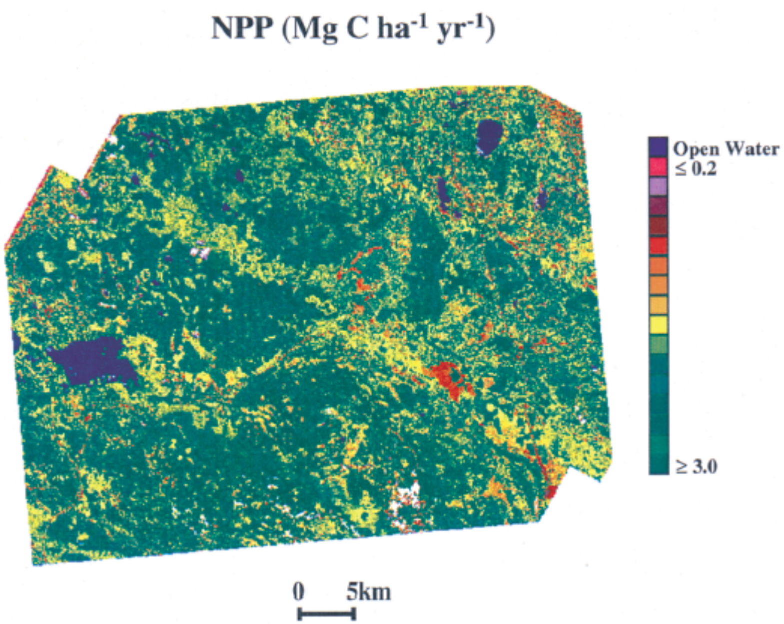

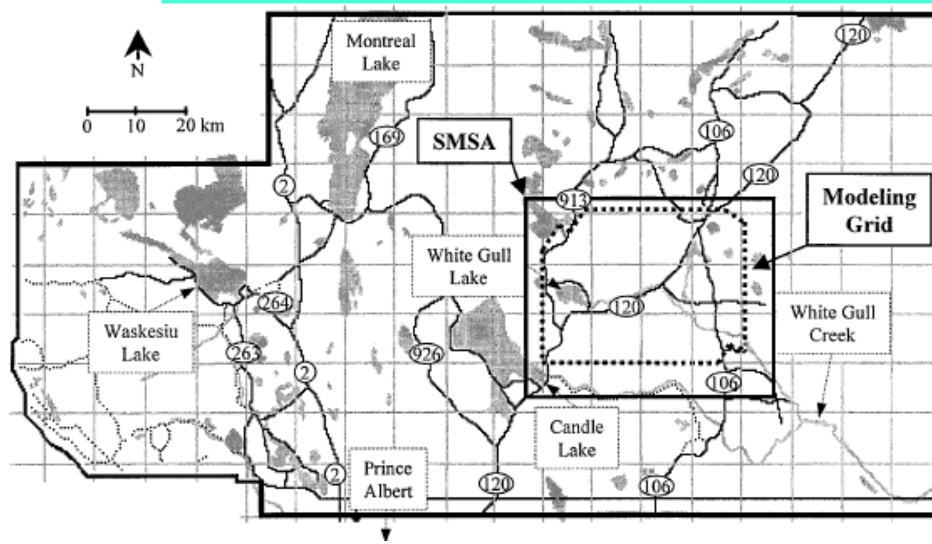

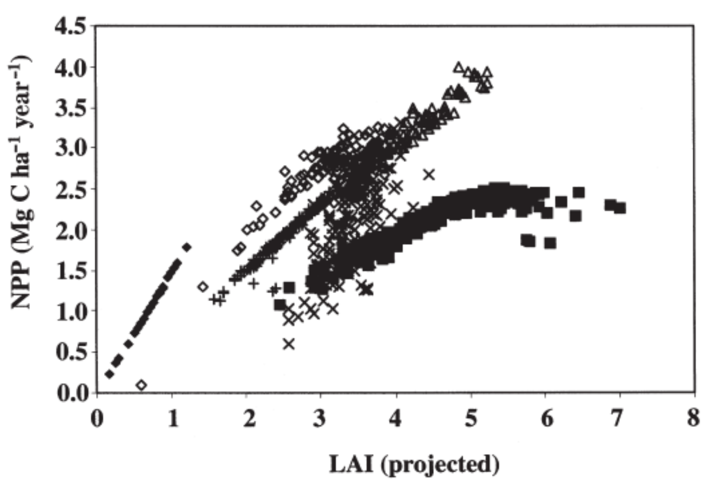

1. Spatial variability was controlled by biomass and LAI variations of fluxes
2. Biophysical differences of broadleaf and needle leaf traits had secondary effects on NPP
3. NPP varied year-to-year due to seasonal variations of climate and 17-22% reduction of NPP observed due to delays in spring thaw.

POST 2020 OBSERVATIONAL STAGE FOR WOODY VEGETATION

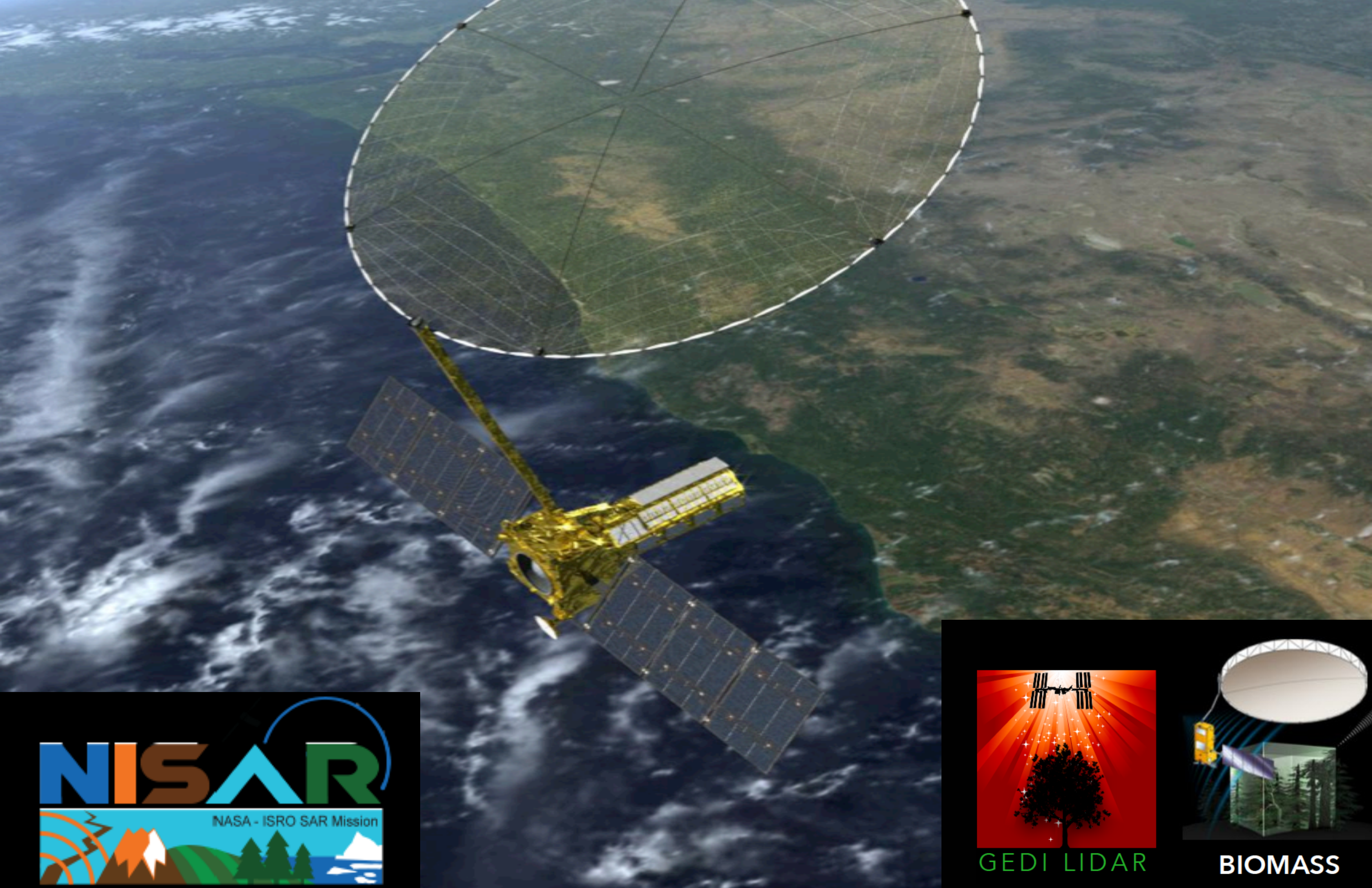

Sensitivity of Radar Measurements to Soil Moisture

Moghaddam, Saatchi, Cuenca, JGR, 2000

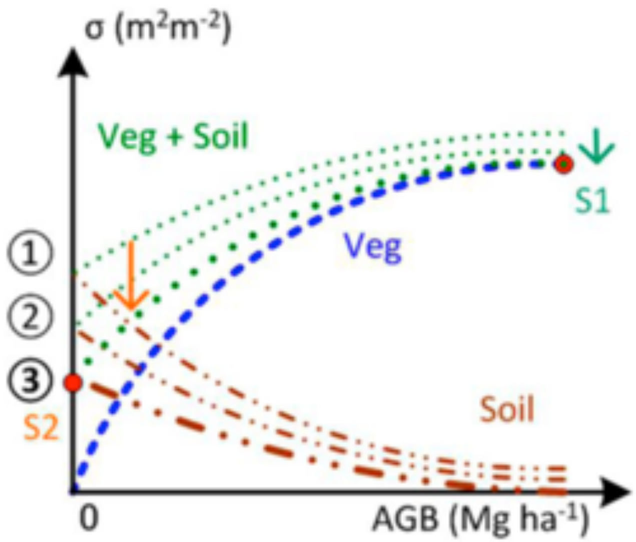

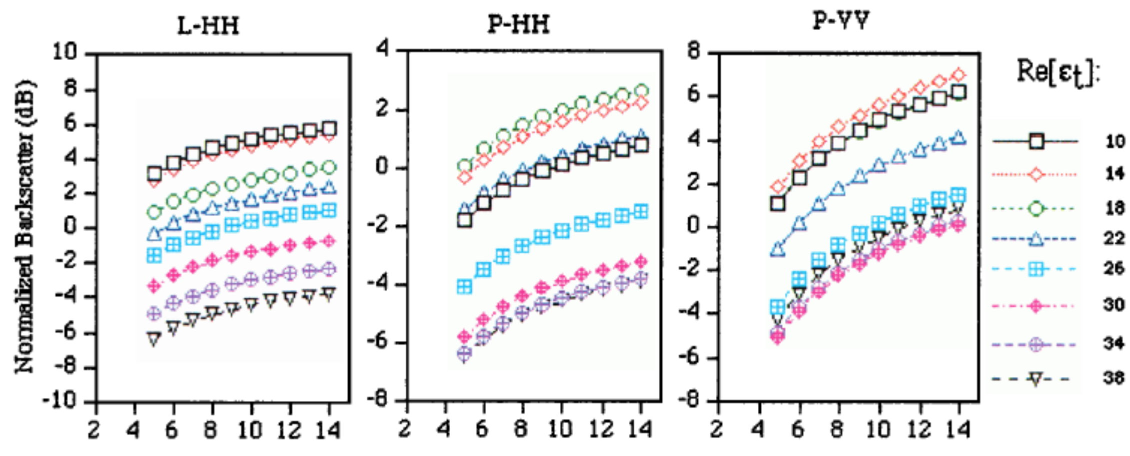

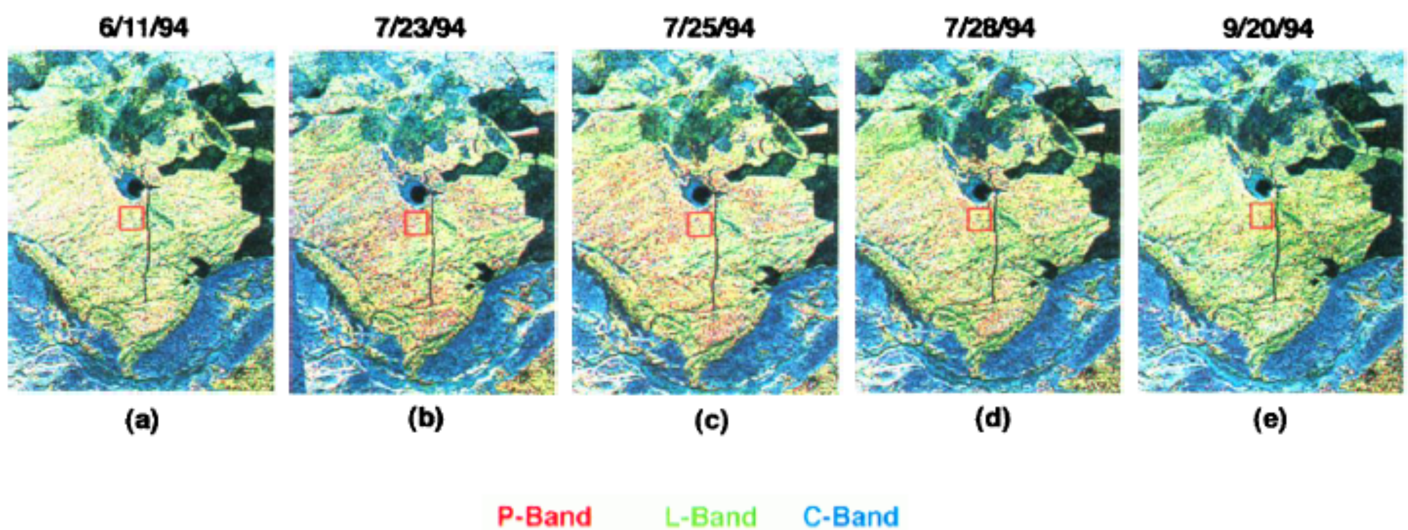

Estimating subcanopy soil moisture with radar

Mahta Moghaddam and Sasan Saatchi
Jet Propulsion Laboratory, California Institute of Technology, Pasadena

Richard H. Cuenca
Bioresource Engineering Department, Oregon State University, Corvallis

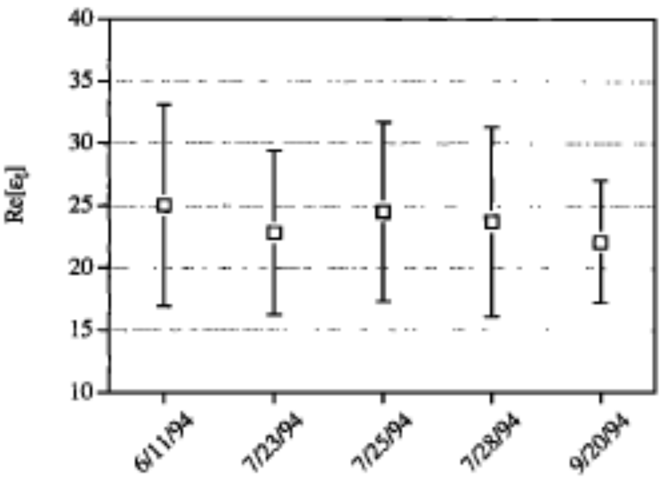

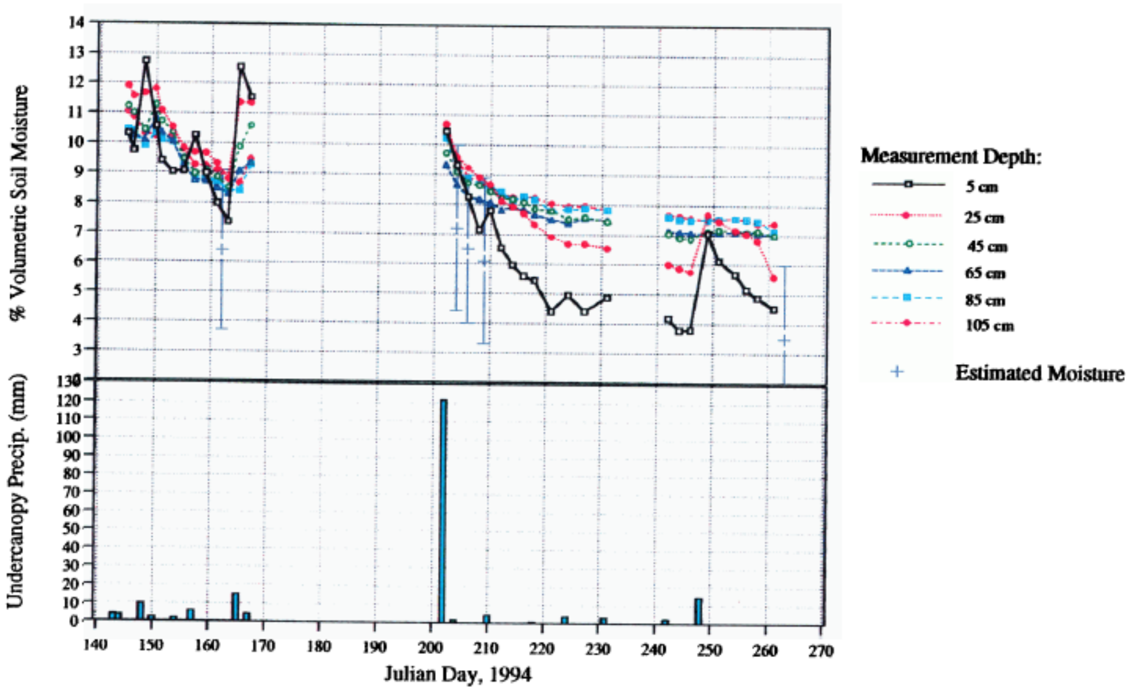

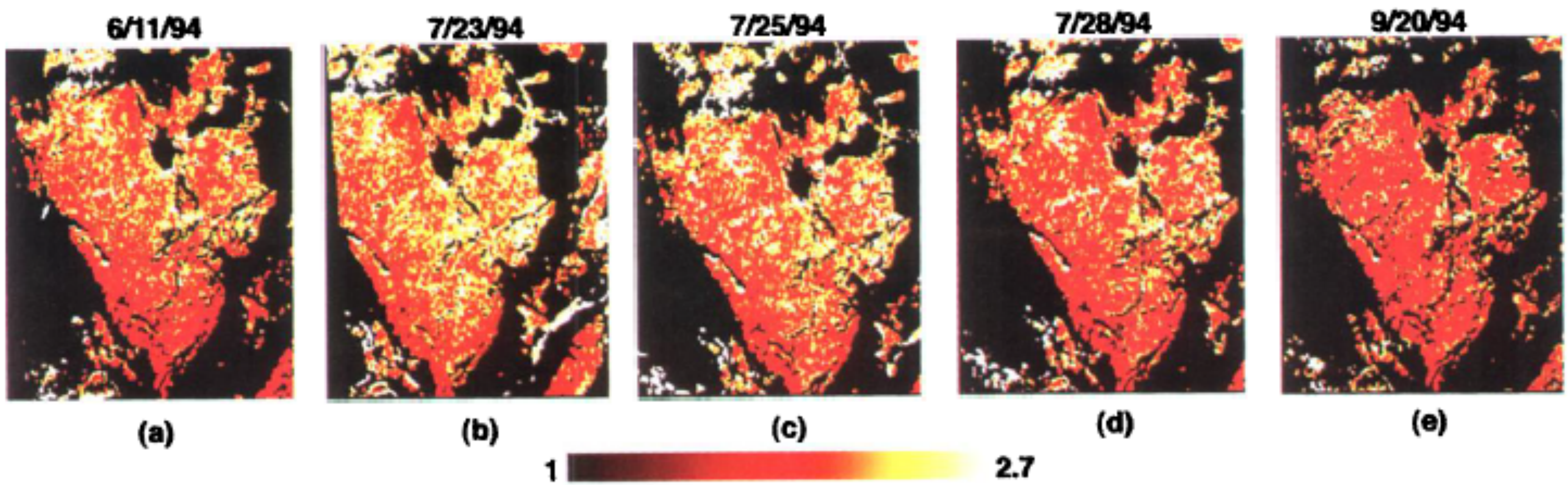

Monitoring Tree Moisture Using an Estimation Algorithm Applied to SAR Data from BOREAS

Mahta Moghaddam, *Member, IEEE,* and Sasan S. Saatchi, *Member, IEEE*

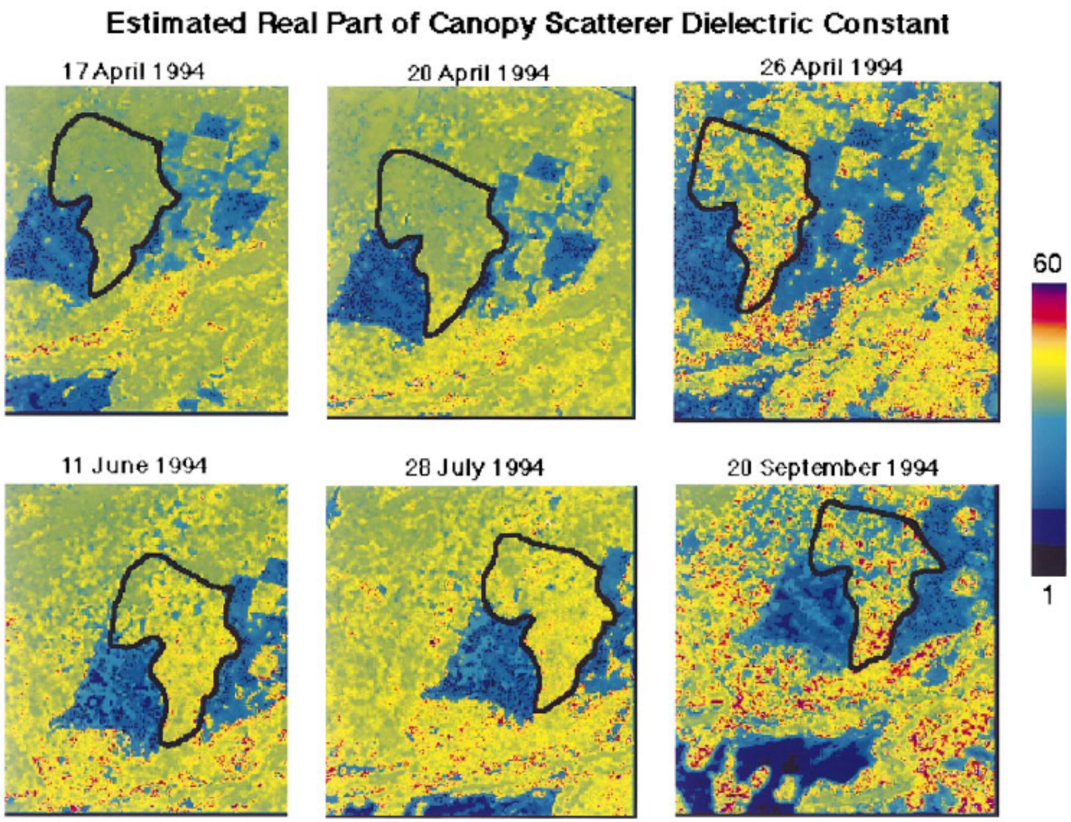

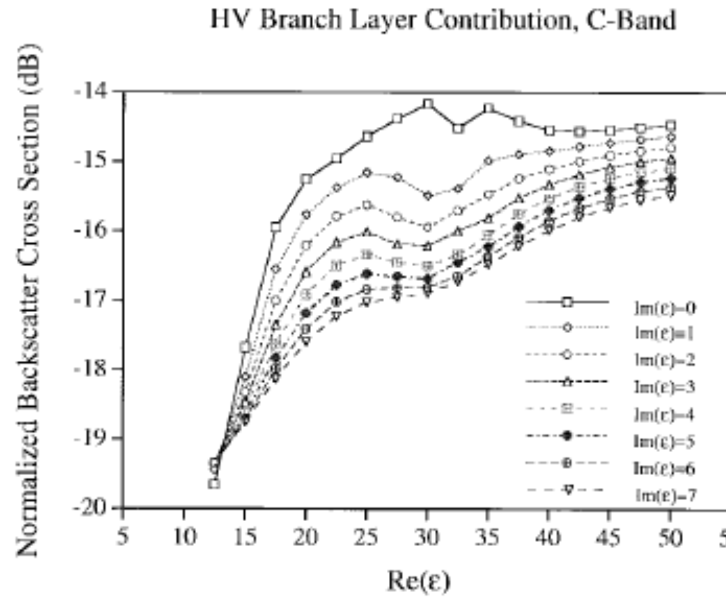

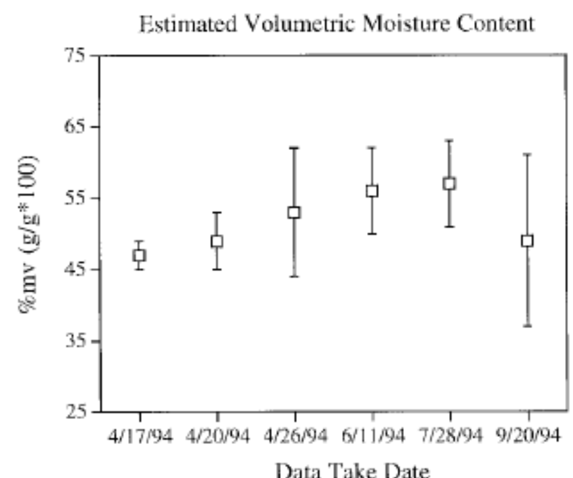

AIRMOSS Earth Venture Mission

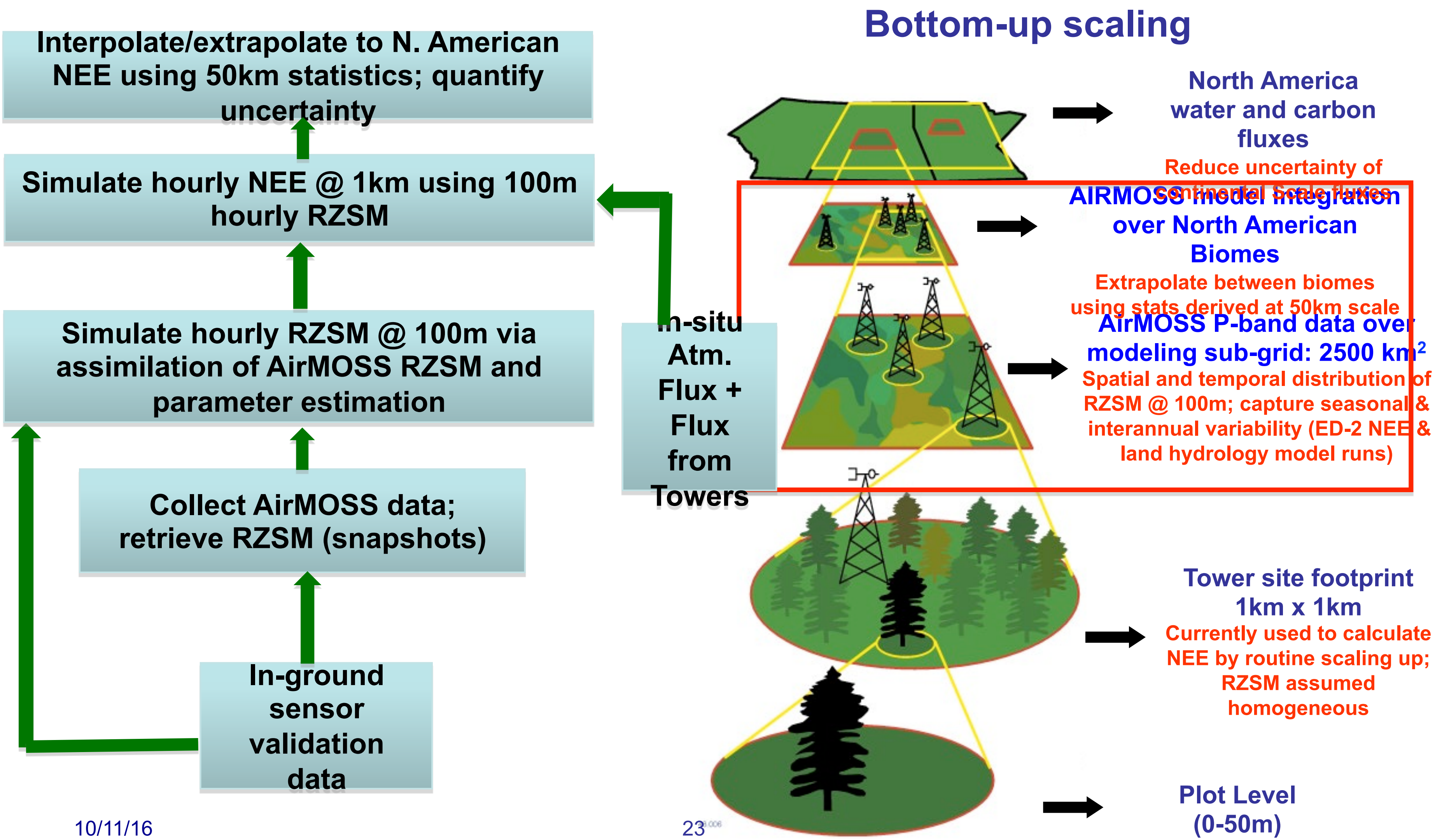

North American Biomes to Cover

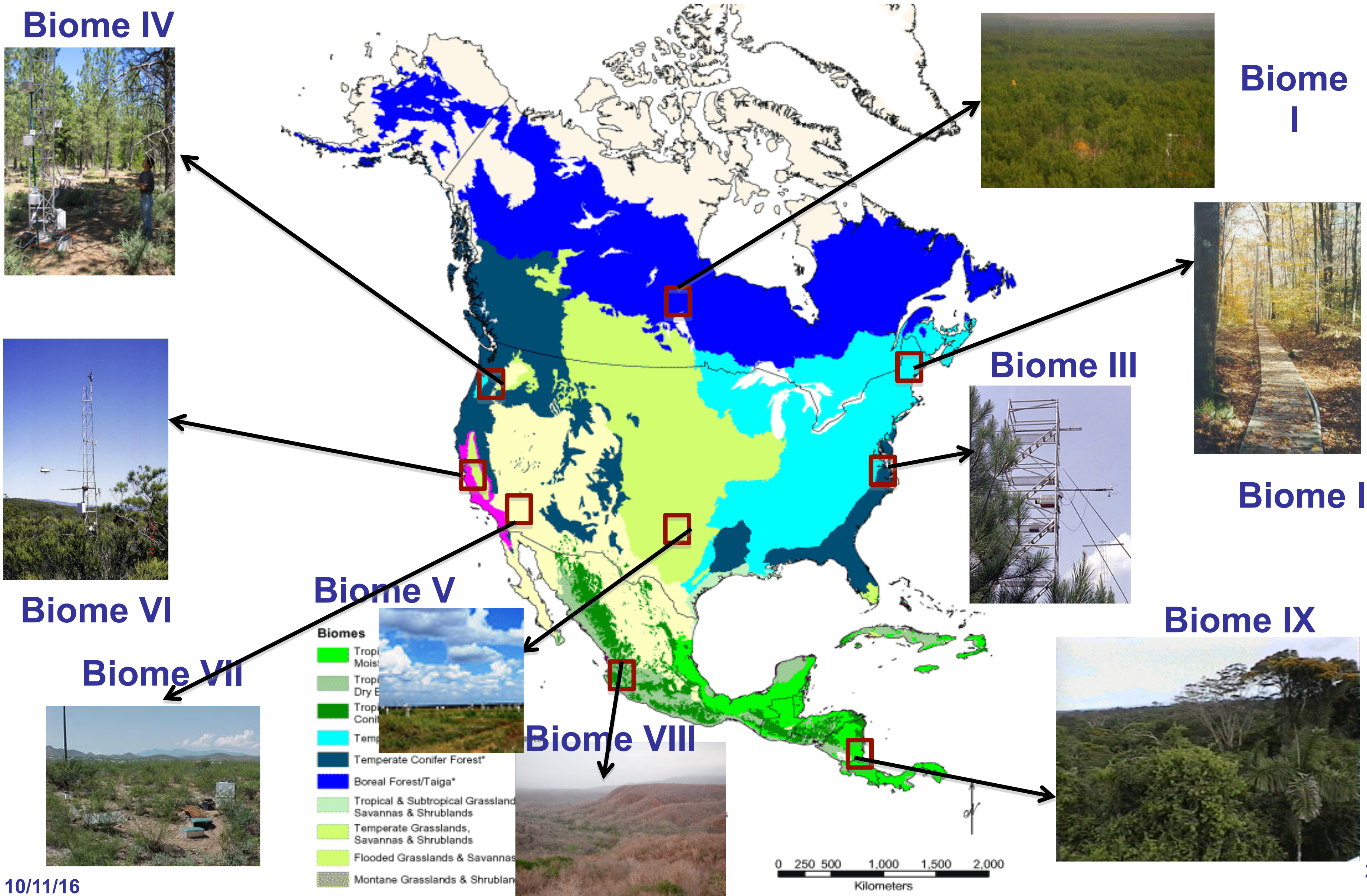

Detection of Areas of Low/Non-vegetated

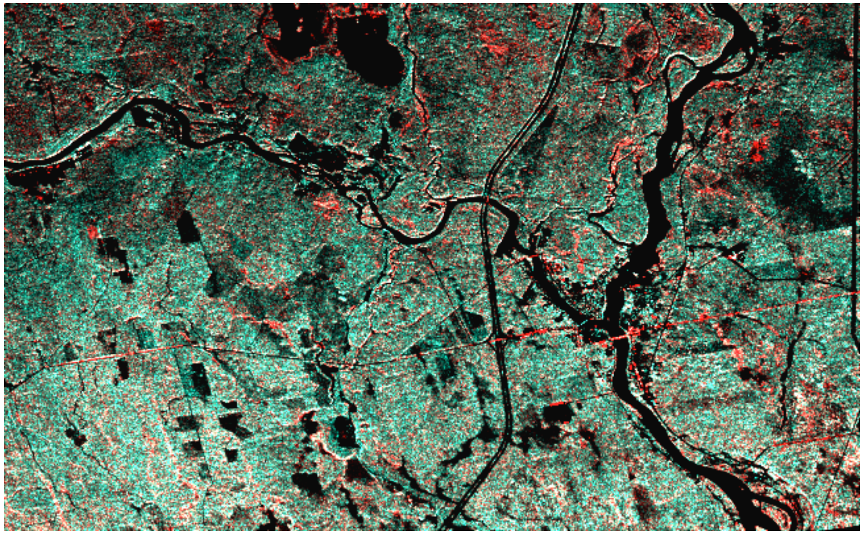

PHH, PHV, PVV

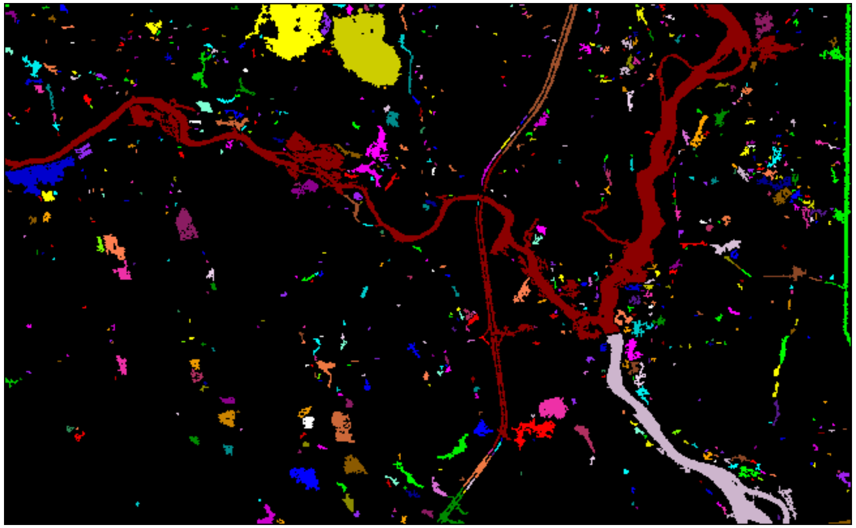

SAR Segmentation

1. **SAR Segmentation provide areas of non or low vegetation at the time of the imagery**
2. **Bare surface algorithm will be applied on SAR segmentated image**
3. **Final inversion algorithm will be applied on a combination of NLCD and SAR segmentation**

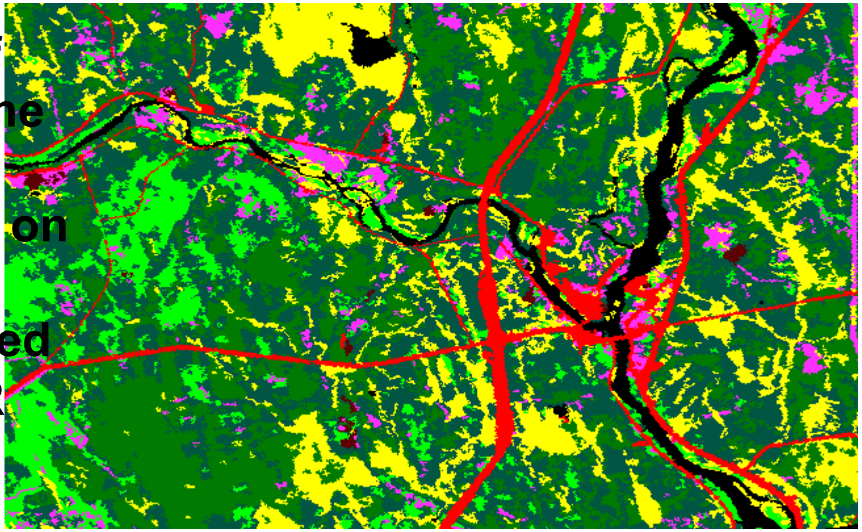

NLCD

Soil Moisture Howland Maine

Aboveground Vegetation Biomass Density (Mg/ha)

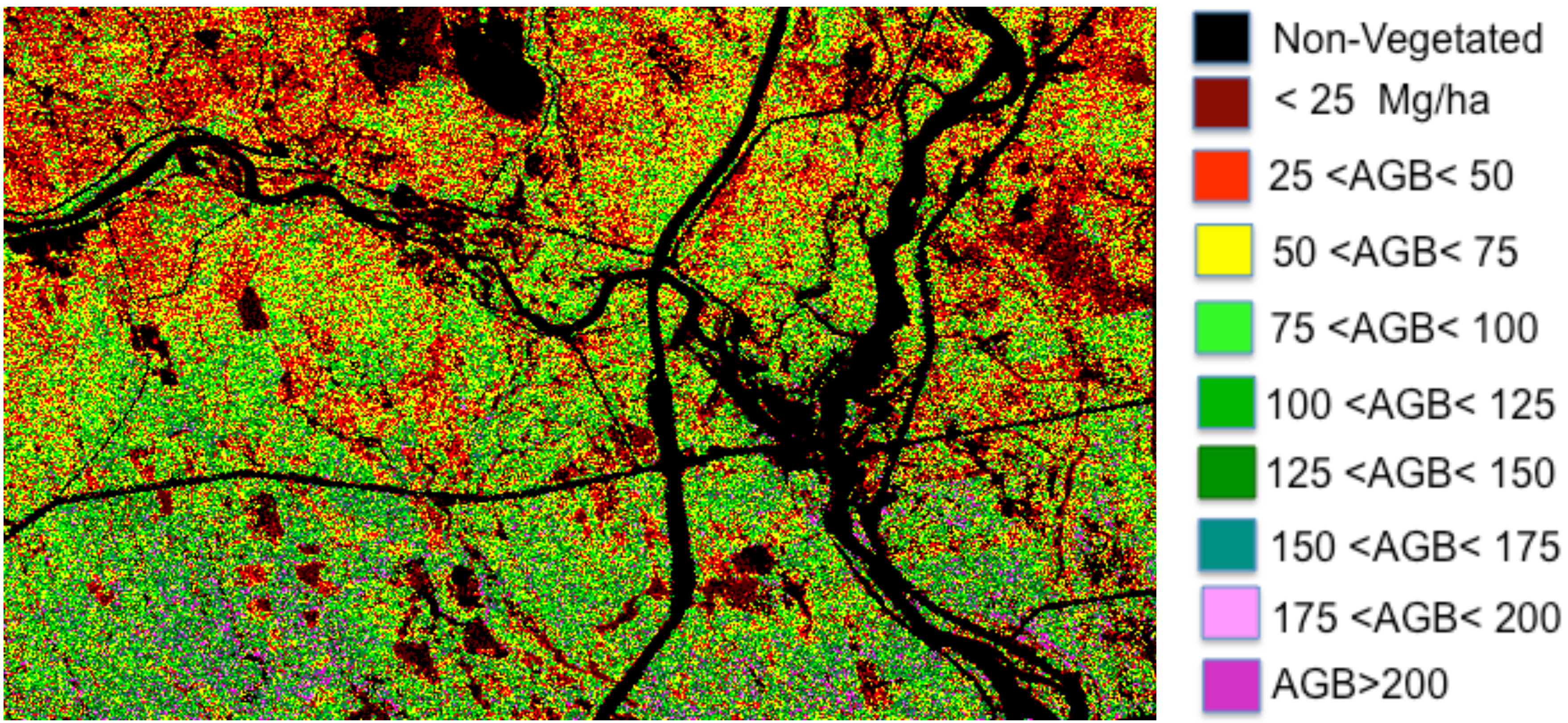

0 < W < 350 Mg/ha

Mean(W) = 64 Mg/ha

Soil Moisture Howland Maine

Soil moisture Map

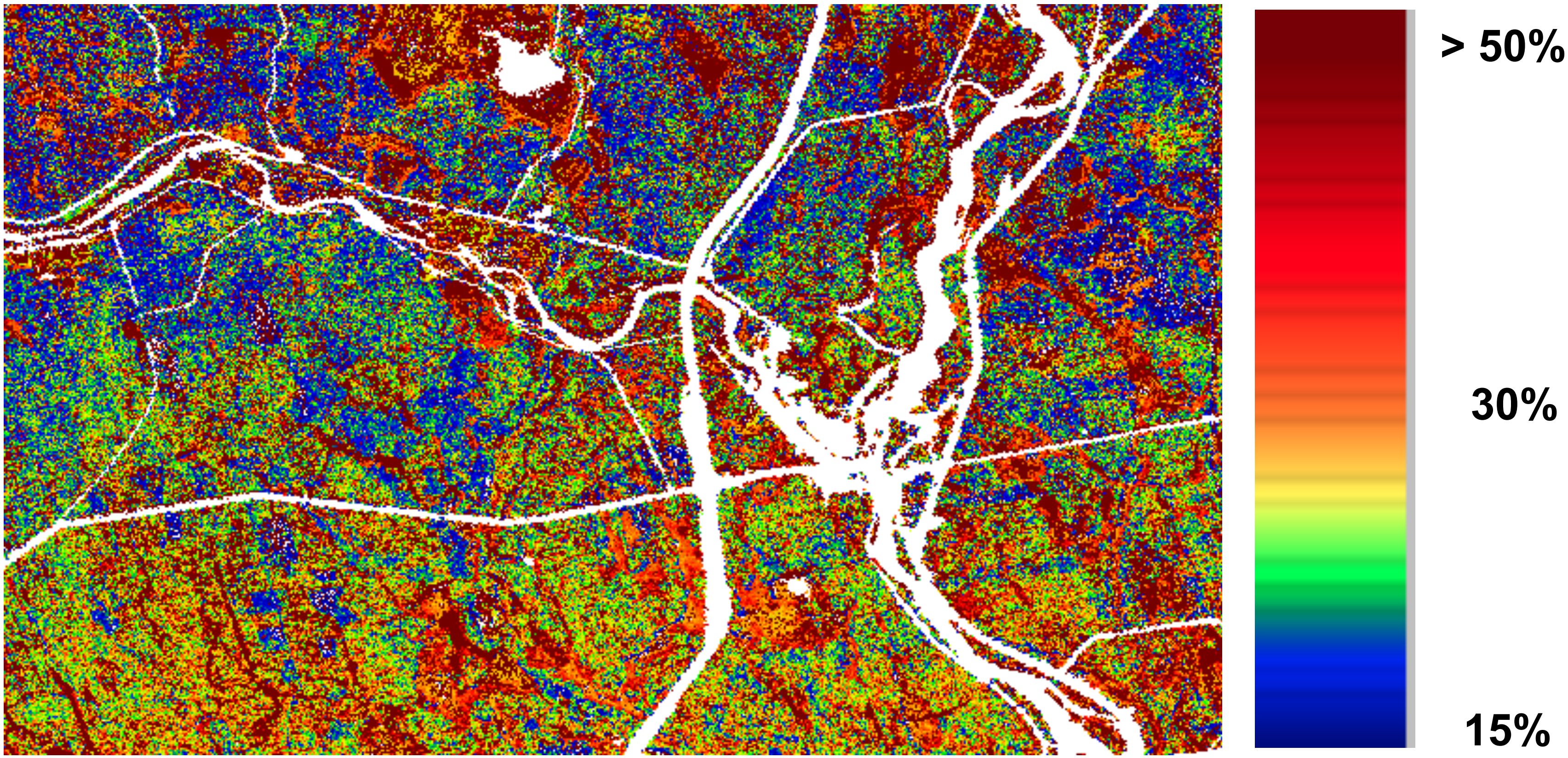

0 < mv < 45%
Mean(mv) = 31.86%
Ground measurement = 28.4%

Soil Moisture Howland Maine

Soil Penetration Depth

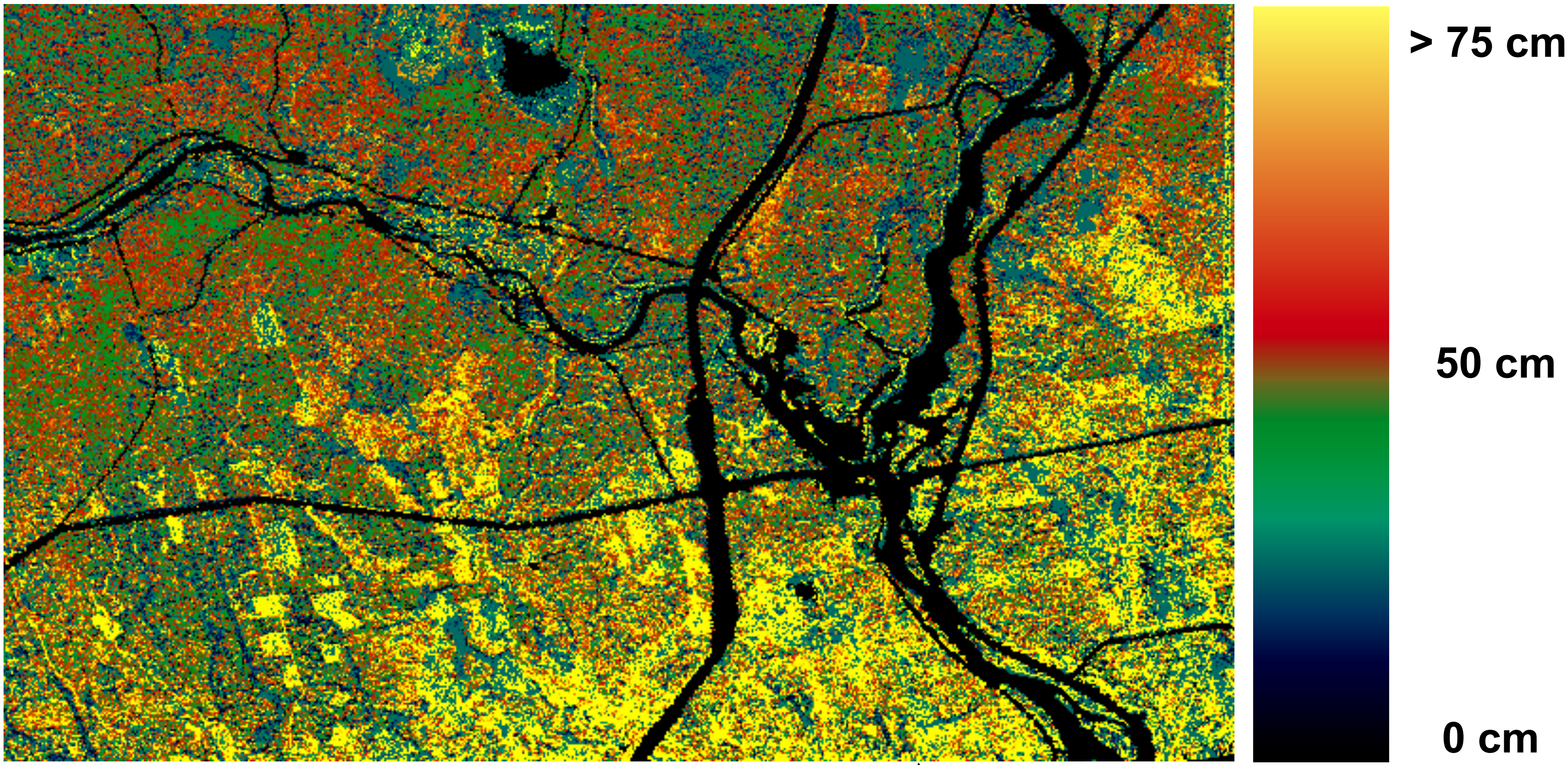

$$d = \frac{-\log_e(0.1)\lambda}{2\pi n_i}; \quad n_i = \mathrm{Im}\left(\sqrt{\varepsilon_r}\right)$$

$$Depth = d\cos\theta_2, \quad \sin\theta_2\sqrt{\varepsilon_2} = \sin\theta_1\sqrt{\varepsilon_1}$$

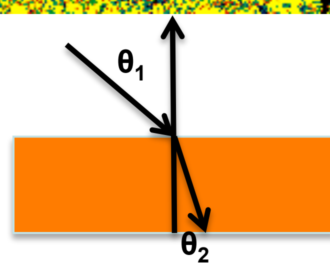

$0 < d < 75$ m

Mean(d) = 50 cm

Measurement of Root-zone Soil Moisture

P-Band Radar Retrieval of Subsurface Soil Moisture

Tabatabaeenejad et al. 2015

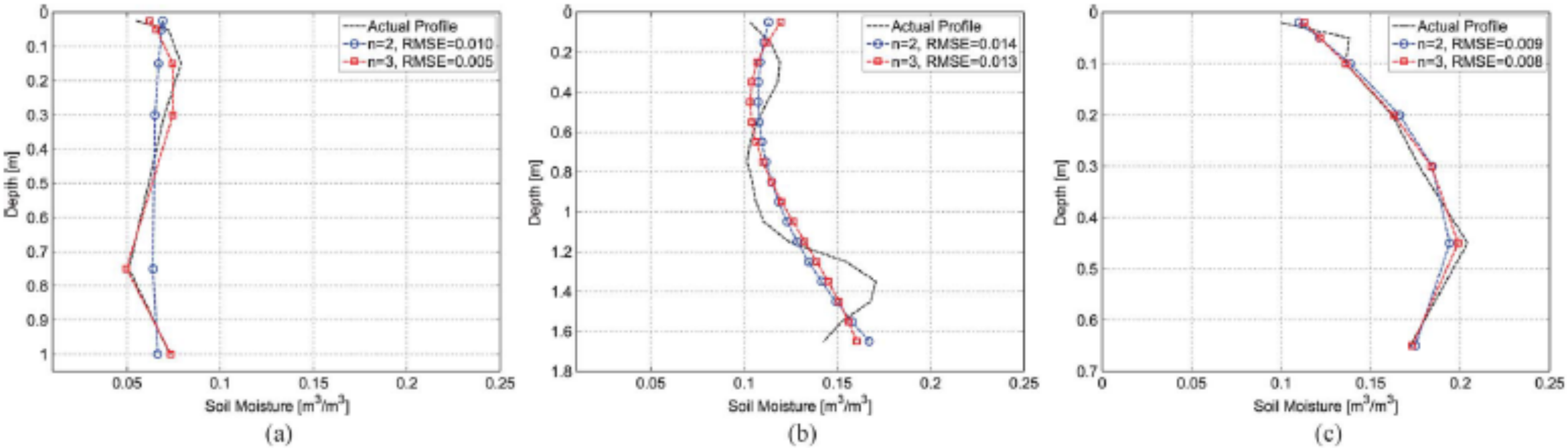

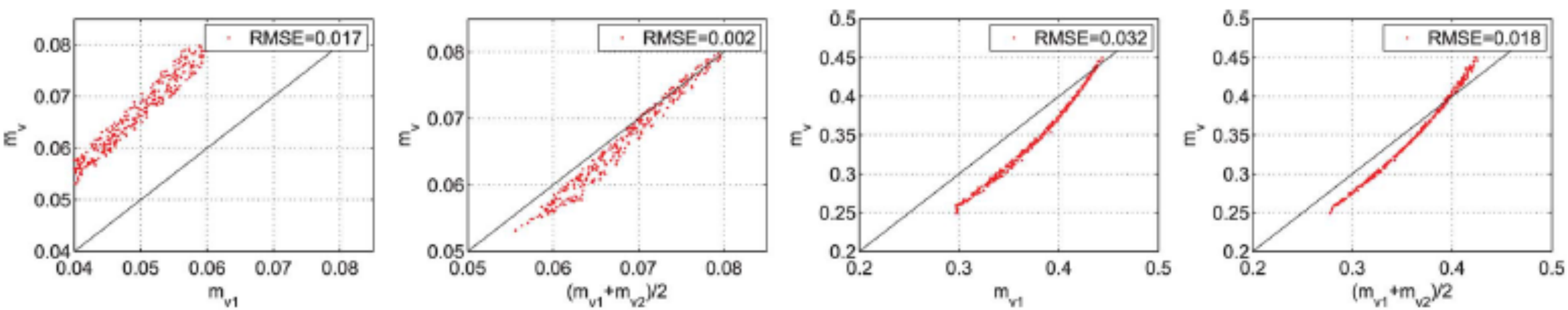

Microwave Observations of Freeze and Thaw of soil and vegetation

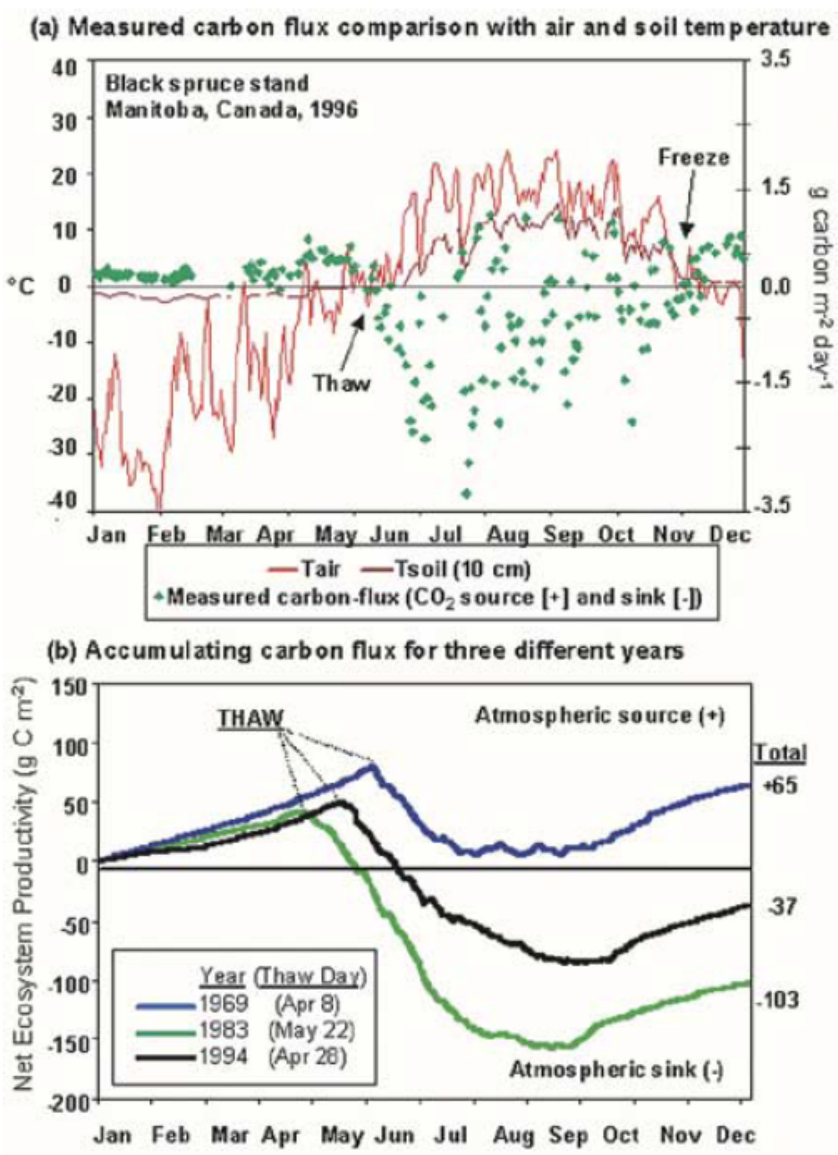

Entekhabi et al. 2004

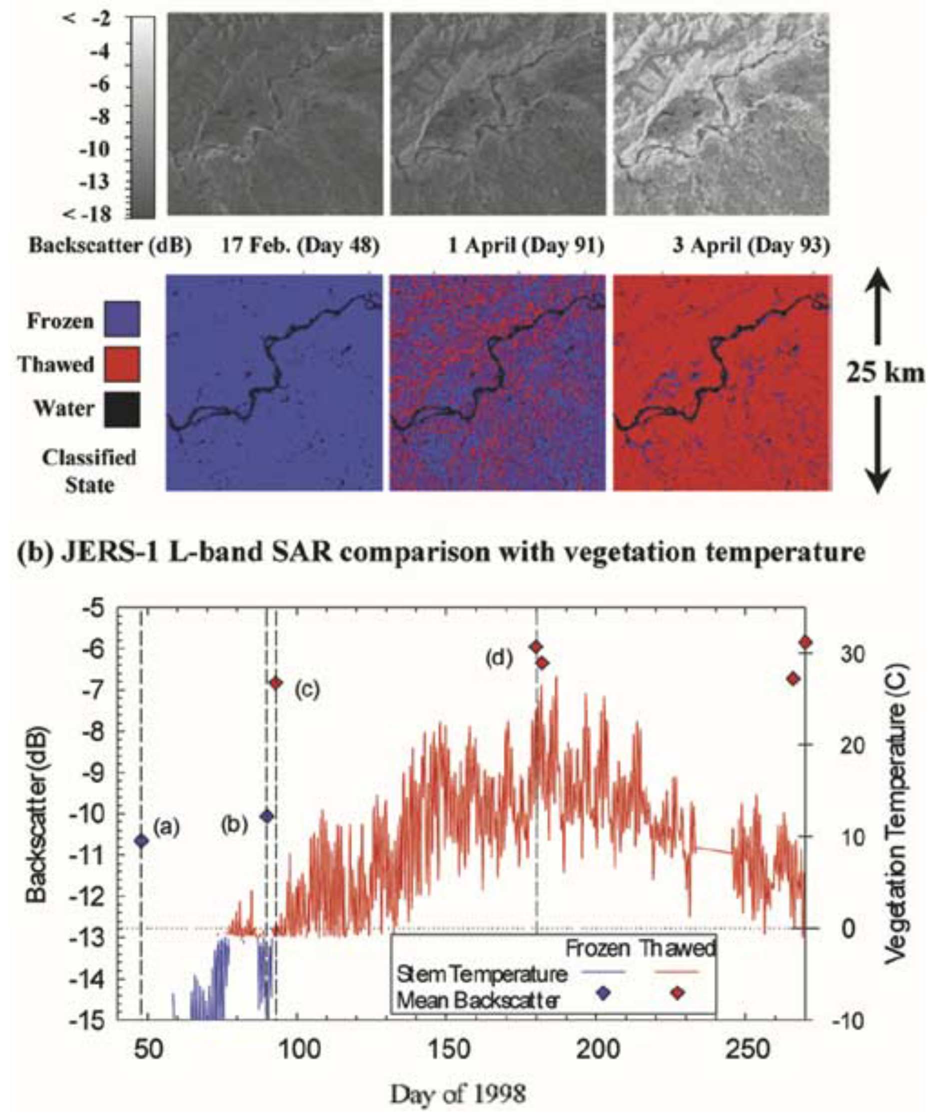


Linking Canopy Physiology to Hydraulics

Monitoring Water Flow in Woody Vegetation by Dielectric Probes

McDonald et al. 1999

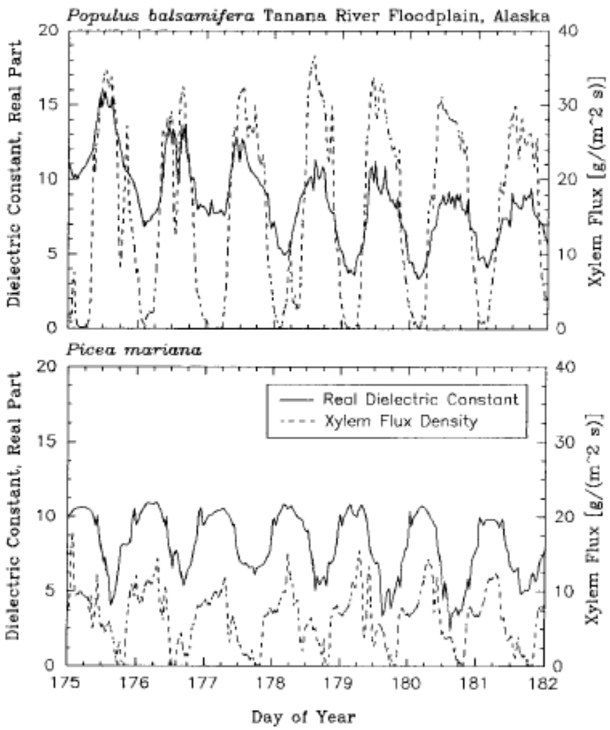

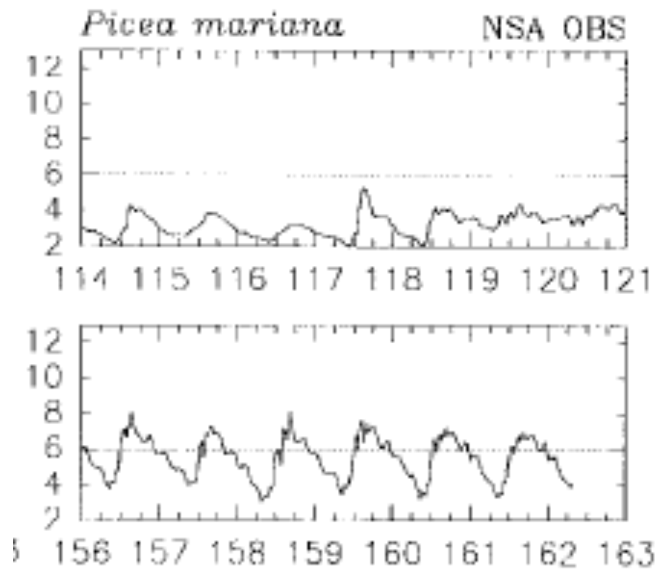

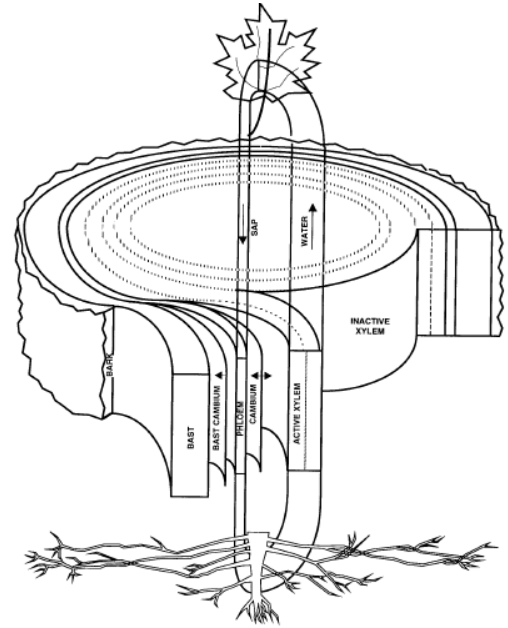

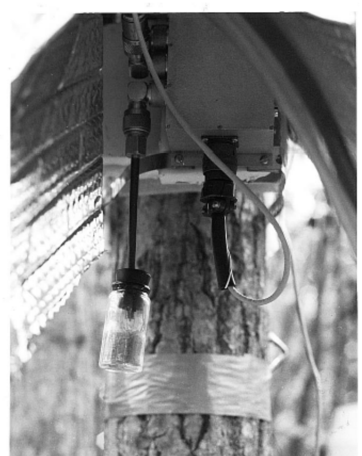

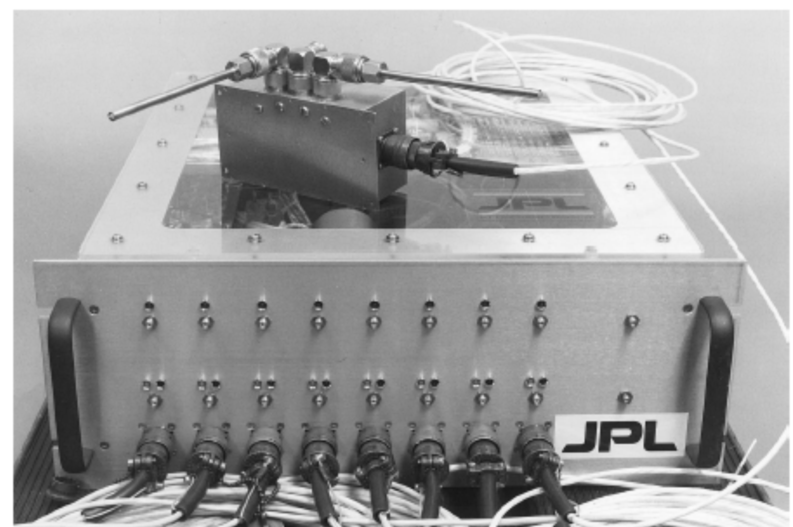

Trends in high northern latitude soil freeze and thaw cycles from 1988 to 2002

Smith, Saatchi & Randerson, 2004

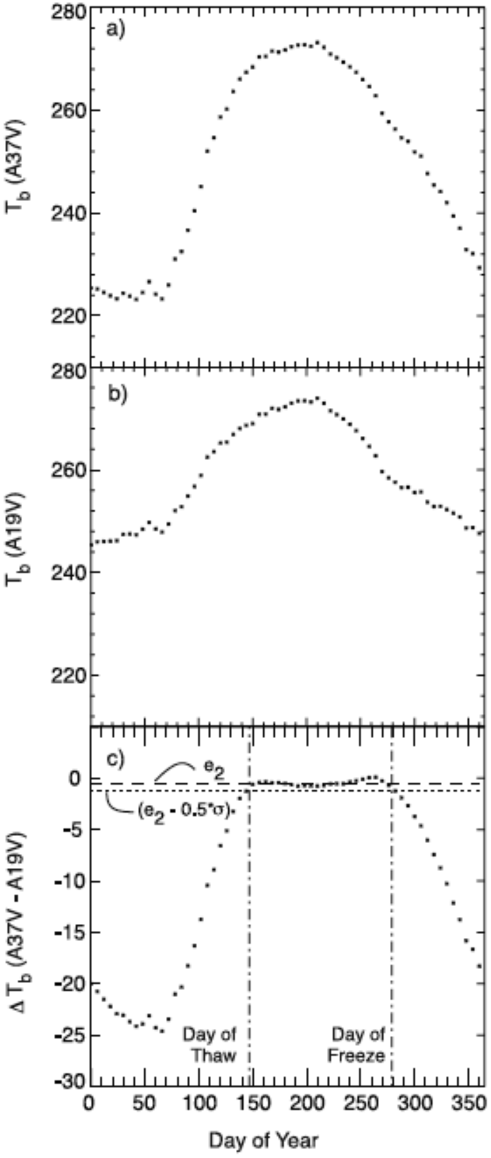

Microwave Radiometer (SSM/I)

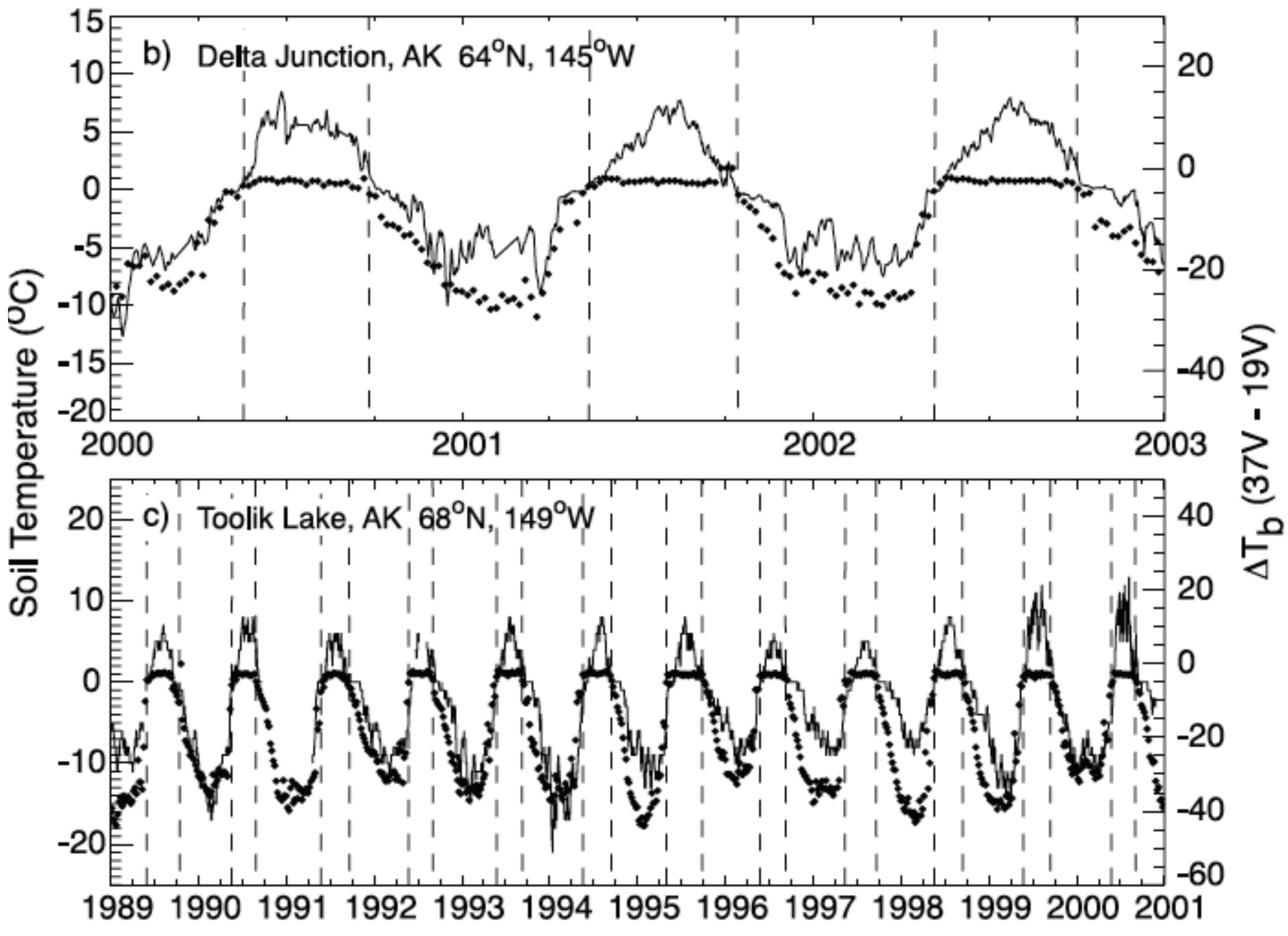

Trends in high northern latitude soil freeze and thaw cycles from 1988 to 2002

Smith, Saatchi & Randerson, 2004

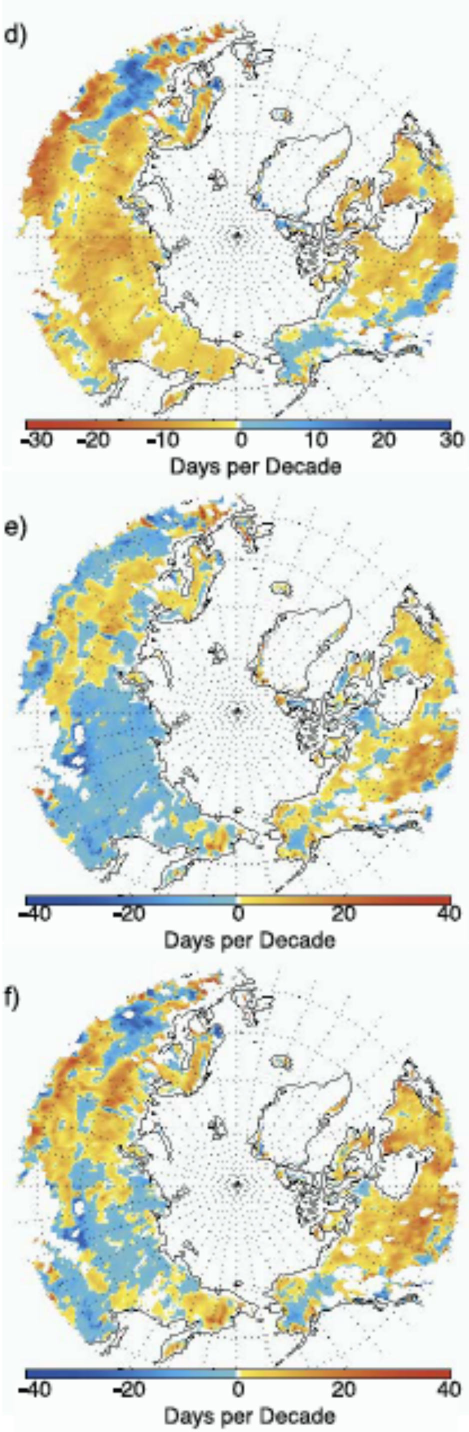

Trend in Thaw date

Trend in Freeze date

Trend in growing season length

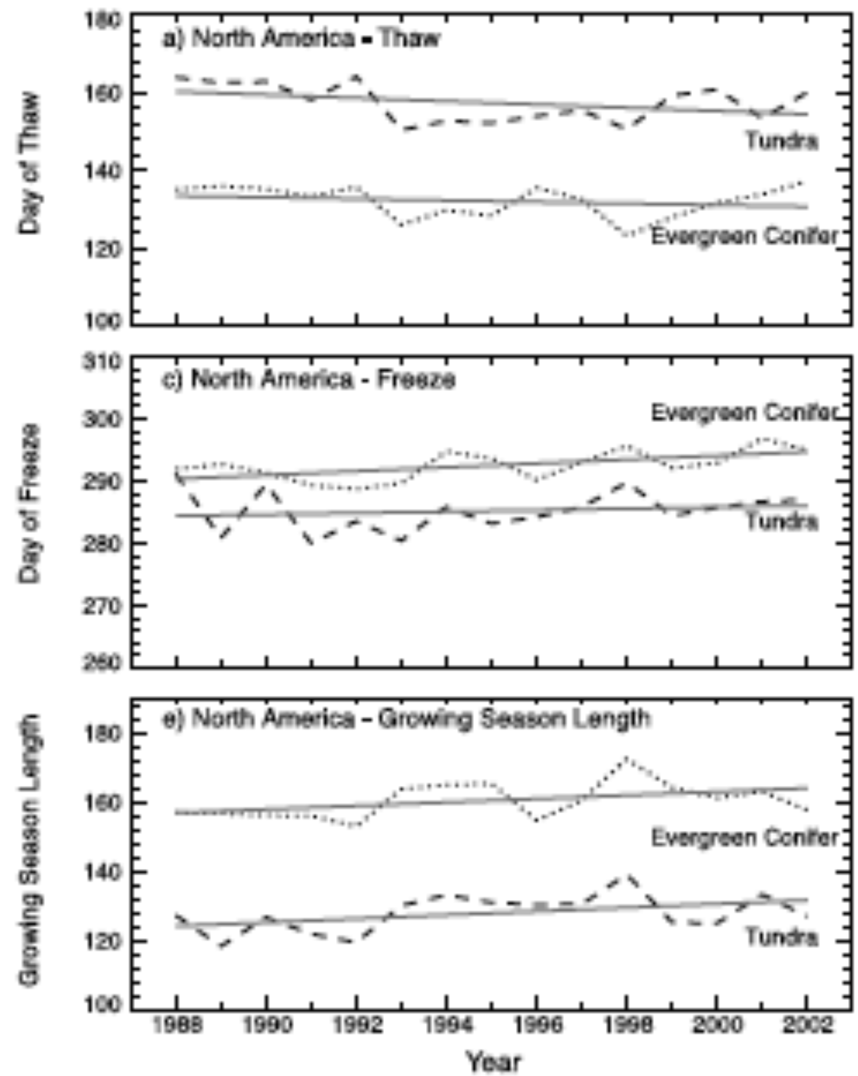

Diurnal & Spatial Variation of Xylem Dielectric Constant

McDonald et al. 2002

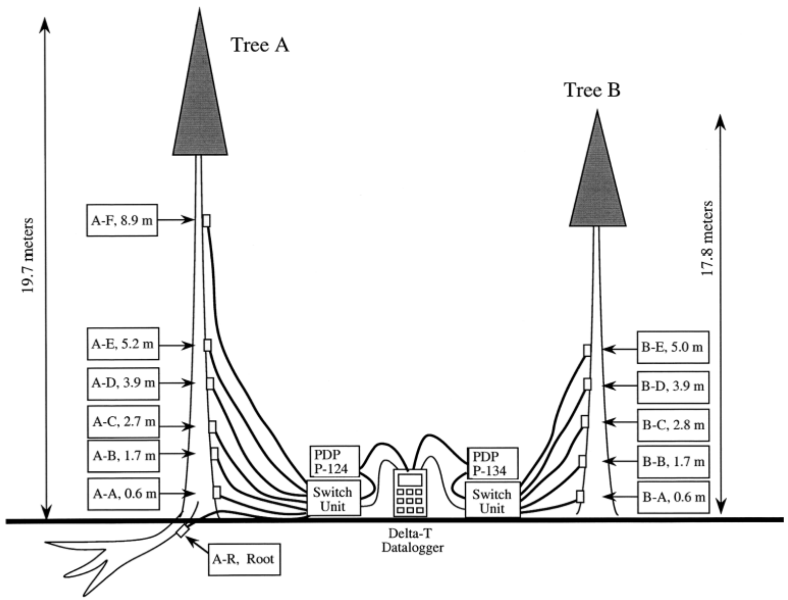

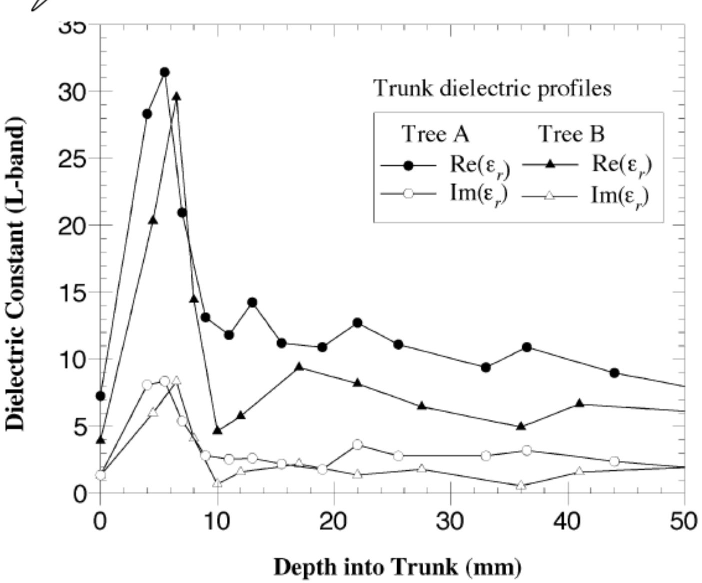

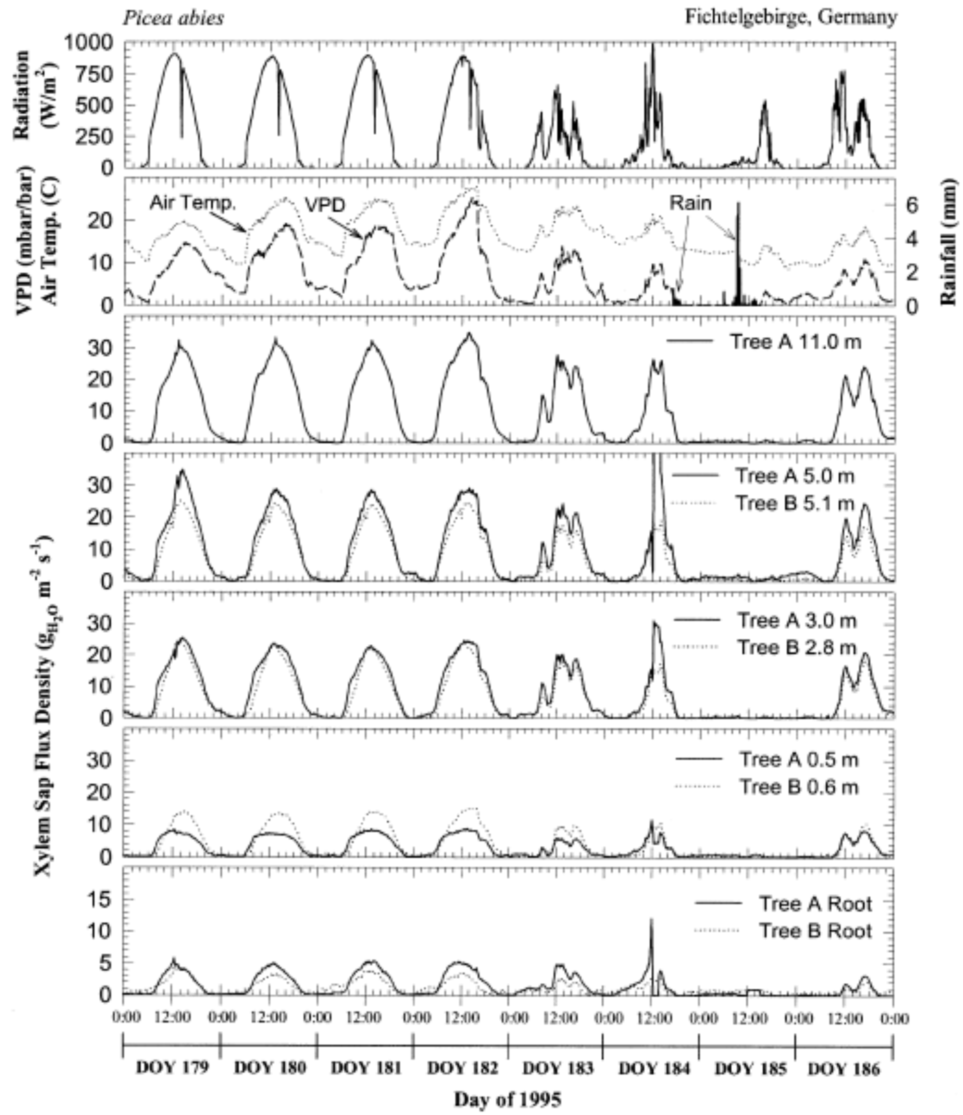

Aquarius and PALSAR

Site I: North Slope

PALSAR and Aquarius

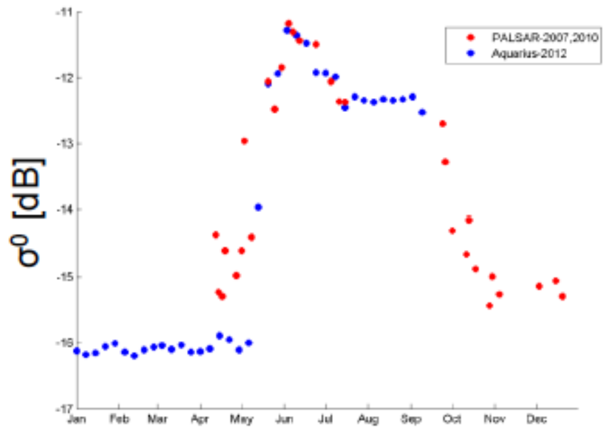

PALSAR – Dominant Landcover Types

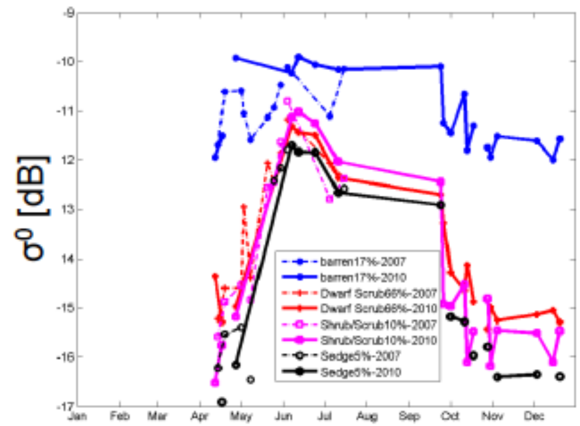

Site II: Interior Alaska

PALSAR and Aquarius

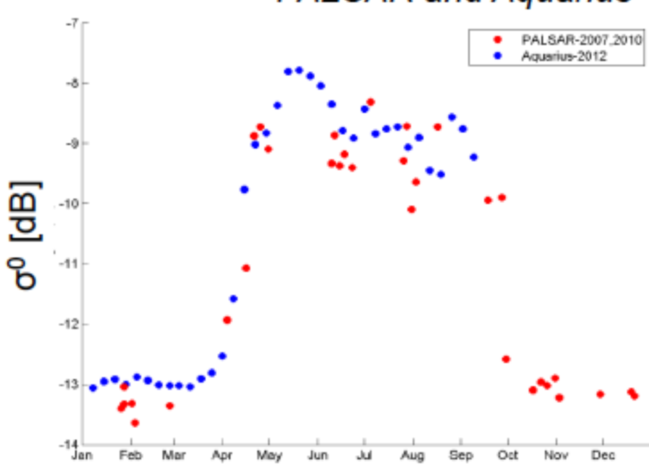

PALSAR – Dominant Landcover Types

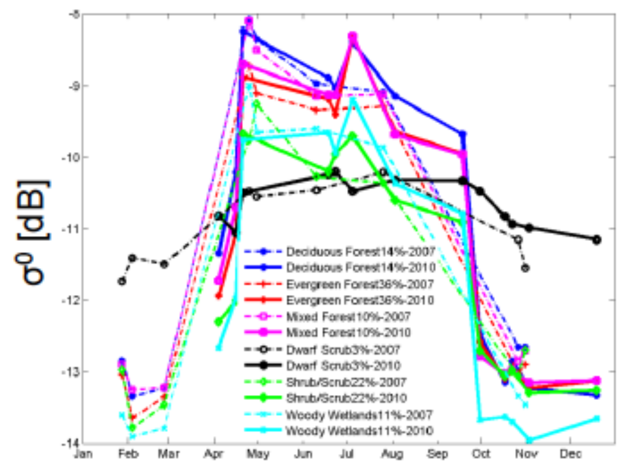

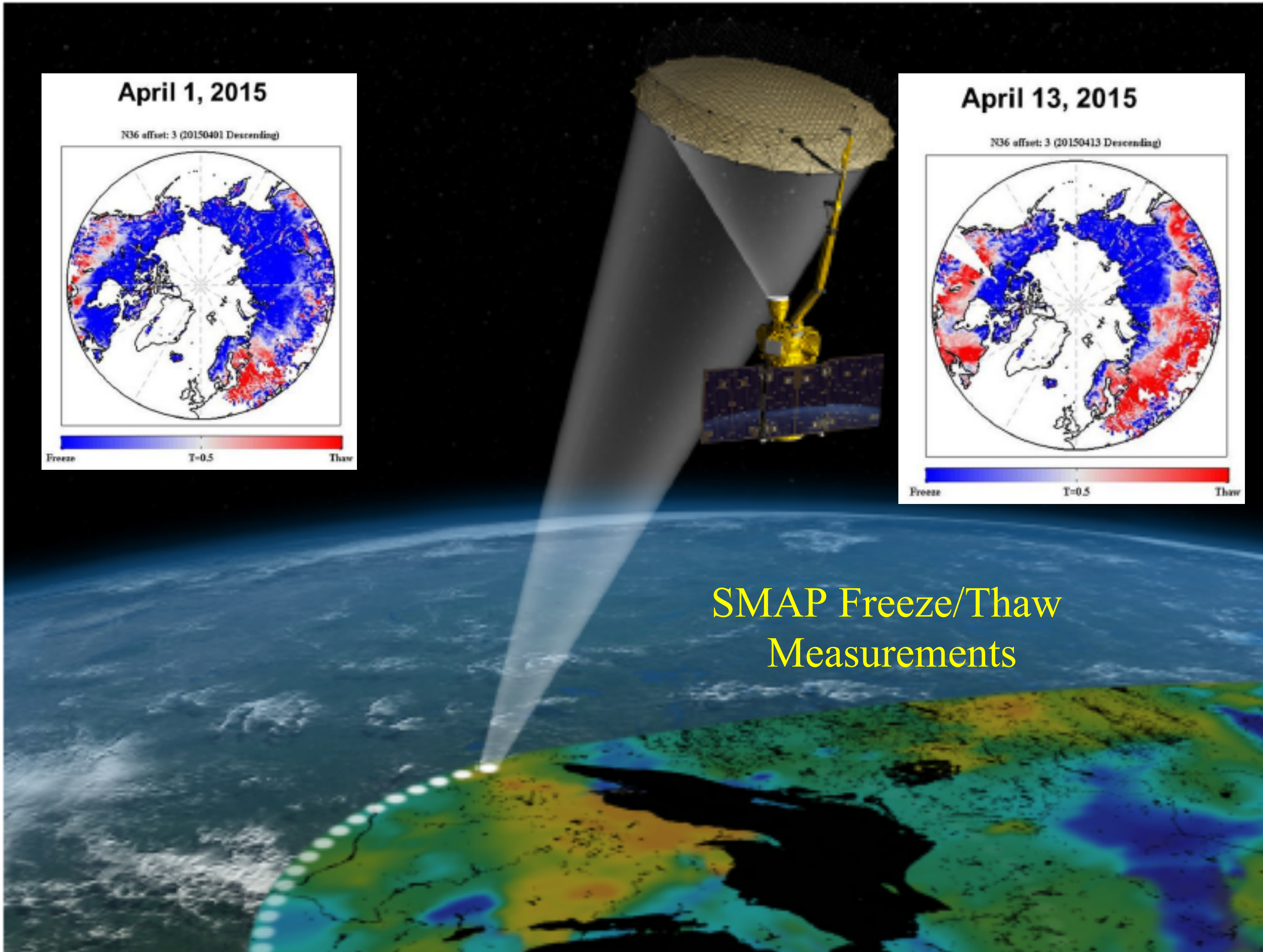
April 1, 2015
N36 offset: 3 (20150401 Descending)
Freeze
T=0.5
Thaw
April 13, 2015
N36 offset: 3 (20150413 Descending)
Freeze
T=0.5
Thaw
SMAP Freeze/Thaw
Measurements

Summary

Return of Variance!

Understand Uncertainty!

Importance of Scaling!

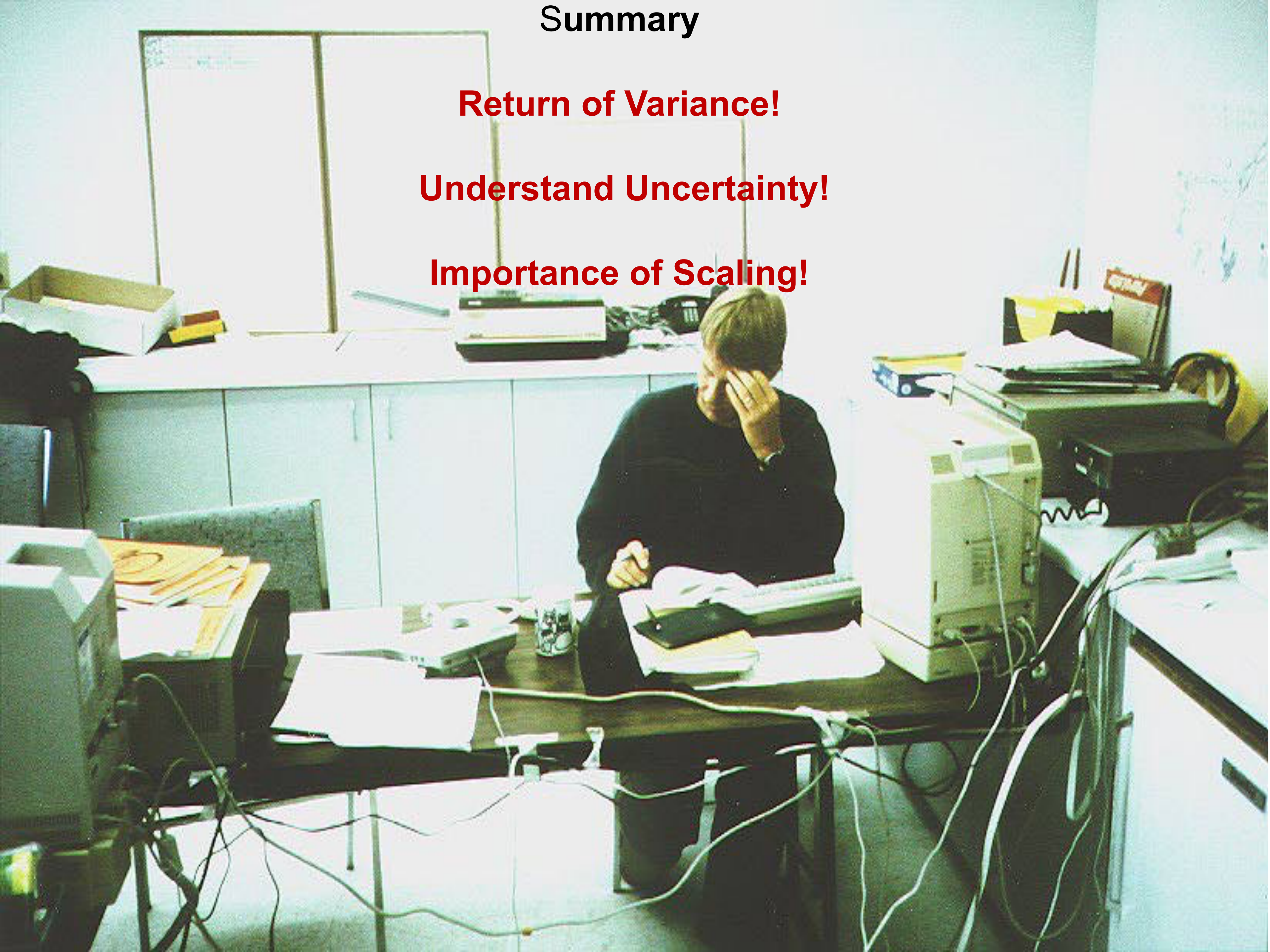

Radar Remote Sensing of the Spring Thaw Transition Across Boreal Landscape

Kimball, McDonald, et al. 2004

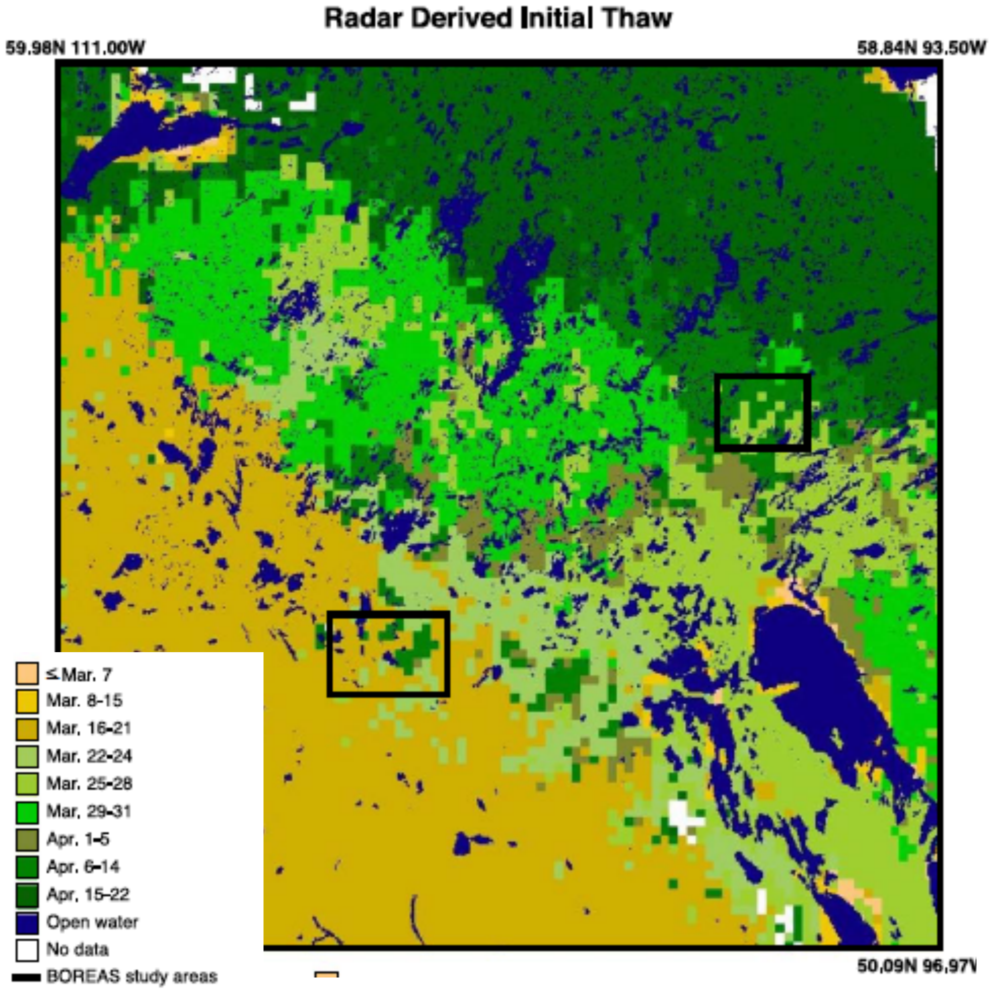

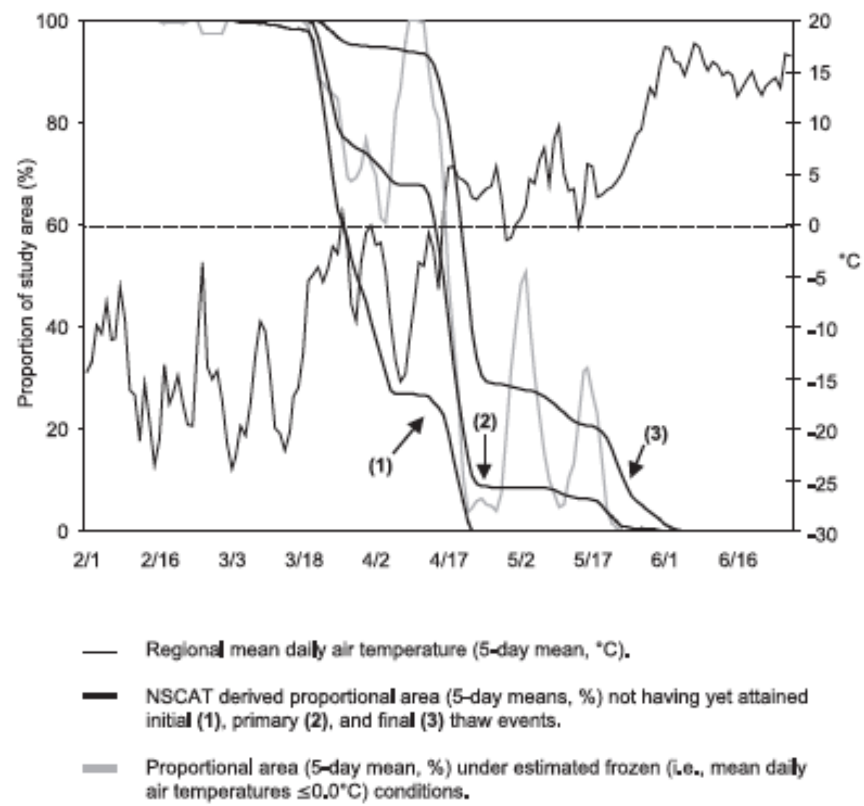

WE HAD NO CLUE!